Title
IR Spectroscopy of Hydrogen Bonded Charged Clusters

Authors
Crofton, M.W.
Price, J.M.
Lee, Yuan T.

Publication Date
1991

LBL-29681

Lawrence Berkeley Laboratory
UNIVERSITY OF CALIFORNIA

Materials & Chemical
Sciences Division

To be published as a chapter in **Clusters of Atoms and Molecules**, H. Haberland, Ed., Springer-Verlag, Publisher, Berlin, 1991

IR Spectroscopy of Hydrogen Bonded Charged Clusters

M.W. Crofton, J.M. Price, and Y.T. Lee

September 1990

Prepared for the U.S. Department of Energy under Contract Number DE-AC03-76SF00098.

DISCLAIMER

LBL-29681

IR SPECTROSCOPY OF HYDROGEN BONDED CHARGED CLUSTERS

M.W. Crofton, J.M. Price, and Y.T. Lee

Department of Chemistry
University of California

and

Materials and Chemical Sciences Division
Lawrence Berkeley Laboratory
Berkeley, CA 94720 USA

September 1990

This work was supported by the Director, Office of Energy Research, Office of Basic Energy Sciences, Chemical Sciences Division, of the U.S. Department of Energy under Contract No. DE-AC03-76SF00098.

5.4 IR SPECTROSCOPY OF HYDROGEN BONDED CHARGED CLUSTERS

M.W. Crofton, J.M. Price, and Y.T. Lee

Department of Chemistry
University of California, Berkeley
and
Materials and Chemical Sciences Division
Lawrence Berkeley Laboratory
Berkeley, CA 94720 USA

5.4.1 General Background and Motivation

"[N]o rest is given to the atoms in their course through the depths of space. Driven along in an incessant but variable movement, some of them bounce far apart after collision while others recoil only a short distance from the impact. From those that do not recoil far, being driven into a closer union and held there by the entanglement of their own interlocking shapes, are composed firmly rooted rock, the stubborn strength of steel and the like..."

-Titus Lucretius Carus, "On the Nature of the Universe", 55 B.C.[1]

The above reference demonstrates that our interest in the forces that hold groups of atoms together is nearly as old as the concept of atoms themselves. Progress in our understanding of the strong interactions that constitute chemical bonds has been considerable, but it has not been until relatively recently that it has been possible to probe the much weaker forces between molecules that give rise to many of the interesting properties of bulk matter. One important approach in the investigation of these forces has been to study cluster systems.

Charged clusters, the subject of this chapter, constitute an important class about which little structural or dynamical information has been measured so far in the gas phase. These species are represented by the generic formula: $A^{\pm q} \cdot L_n$, where $A^{\pm q}$ is most commonly a singly charged ion and L_n are the surrounding n neutral ligands. A large body of data is available concerning the thermodynamics and kinetics of these species however, (see chapters 5.5-5.9, 5.11) and Castleman in addition to his own contributions has compiled the thermodynamic results of many investigators into an atlas,[2] listing the ΔH°, ΔS°, and ΔG° of individual clustering steps for a wide range of ions.

Structural information about charged clusters can sometimes be found by mapping ΔH° as a function of cluster size. Performing this operation can yield a curve with discontinuities at masses where the ion's first solvation shell can reasonably be expected

to fill. This is the case for the ammoniated ammonium ion, $NH_4^+(NH_3)_n$, where a strong discontinuity is observed between n=4, the complete first solvation shell, and n=5. A discontinuity is not obvious for the hydrated hydronium ions, $H_3O^+(H_2O)_m$, which have quite high binding energies even for second shell ligands and whose first shell is filled at m=3. (See Table I.) Although these measurements can give qualitative information about the location of the solvent molecules around the ion, and geometries can be calculated from ab initio methods[3], the accurate equilibrium geometry of a given cluster can still only be obtained from spectroscopic measurements.

In nature, gas phase ionic clusters are abundant in cold environments with ionizing particles or photons present, including interstellar space and the earth's atmosphere.[4,5] It is known from mass spectrometer studies, for example, that the hydrated hydronium ($H_3O^+(H_2O)_n$) species are the dominant ions in some regions of the atmosphere.[6,7] Ionic clusters play essential roles in atmospheric chemistry,[8] nucleation[9] and biology,[10] and are important components of many solutions and crystalline materials. Ions in solution can be thought of at some level of approximation as a collection of ionic clusters.

Charged clusters generally have a higher binding energy than their neutral counterparts. For the small species with n=1, binding energies similar to those of weak covalent chemical bonds are not uncommon:[2] ΔH° is $\approx$ -36 kcal/mole for the reaction $H_3O^+ + H_2O \rightarrow H_5O_2^+$ [11,12] and $\approx$ -27 kcal/mole for the reaction $OH^- + H_2O \rightarrow HOHOH^-$.[13,14] For Li^+ ions solvated by H_2O and a variety of basic ligands, the binding energy is extremely high, often 60 kcal/mole or even more.[2,15,16] Because of the small size of the Li^+, the ion dipole interaction energy is unusually large, and interactions arising from polarization effects can play a considerable role as well. Binding energies for a number of the ionic clusters discussed in this chapter appear in Table I.

Among charged clusters, those species involving hydrogen bonds are of particular importance. Hydrogen bonded species are among the most strongly bound ionic clusters. The strongest hydrogen bond measured in nature, that of FHF^-, has a dissociation energy of 58 kcal/mole[17] or 2.5 eV, weaker than the average covalent bond but well within the range of covalent bond energies. As one of the most ubiquitous interactions in chemistry, the hydrogen bond is profoundly influential in determining the structural organization and processes that occur in a variety of environments, from hydrogen bonding solvents to entire living organisms. The proton transfer reaction,[18,19,20,21,22,23] perhaps the most general and important reaction in chemistry, is governed in hydrogen bonding solvents by hydrogen bonded "cluster" species.

A great many studies have been made of the solvated proton in the liquid and solid phases, using x-ray and neutron diffraction, infrared and nuclear magnetic resonance (NMR) spectroscopy and other techniques.[18,23] While much has been learned from these studies, the presence of a distribution of species in the sample, the impossibility of studying most samples at very low temperatures and other problems, often result in serious ambiguities in data interpretation. Particularly in solution, the structures of $H_3O^+(H_2O)_m$ have not been well understood. In the solid phase, convincing evidence for $H_5O_2^+$ with a centralized bridging proton and $H_9O_4^+$ with C_{3v} symmetry have been found. Many ammonium salts such as the series $NH_4^+X^-$ and $NH_4^+(NH_3)_nX^-$, where X = Cl^-, Br^-, I^- have well-characterized vibrational spectra.[24] The solid phase results, however, are difficult to extrapolate to the liquid or gas phase.

In spite of the substantial effort devoted to the study of the solvated proton in the bulk phases, predictions of the structures and dynamical processes relating to hydrogen bonded systems are often unreliable or computationally intractable.[25,26] For larger systems, it is usually impractical to attempt any detailed predictions. Hydrogen bond lengths, the distance between the X atoms in X-H···X, and stretching frequencies are in general far less accurately determined for cluster systems than for molecules of similar size and type but containing only covalent bonds. This is due in part to the flatness of the potential well even near the bottom, and the greater anharmonicity of the potential surface associated with the hydrogen bond. There is a need for experimental data from which accurate potential surfaces can be derived, in order to guide theoretical efforts.

The understanding of neutral hydrogen bonded systems has been considerably enhanced recently by the detailed spectroscopic studies of species such as $(H_2O)_2$,[27,28,29] $(NH_3)_2$,[25] and a host of van der Waals complexes.[30,31] From these, accurate equilibrium geometries can be determined. While some low resolution data exists for a few of the larger clusters of $(NH_3)_n$[32] and $(H_2O)_n$,[33,34,35] which are of direct interest to the question of the onset of the liquid state, these systems have resisted detailed analysis. The study of these neutral cluster species is complicated experimentally by difficulties in obtaining the spectrum for a given solvation number n without contributions from clusters of different sizes.[32,36] This is due to the lack of an unambiguous technique for mass selection, which is not a problem for charged clusters. The spectroscopic study of hydrogen bonded ionic clusters can answer many of the same questions about hydrogen bonding as similar studies of neutral clusters and further sheds light on the topics of proton transfer and the solvation of ions in solution.

5.4.2 Some Previous Studies:

While there are many attractive features to the study of ionic clusters, including the potential for mass selectivity and the abundance of data on the stepwise heats of formation for the clusters, there is one significant drawback for the spectroscopist: low number density of the sample for study. Due to space charge effects, the production of ions in abundance higher than about $10^{12}/cm^3$ becomes difficult to maintain. While this concentration is certainly sufficient for the spectroscopic study by direct absorption of many molecular ionic species,[37] the production of ionic clusters requires a relatively gentle environment. As in the case of neutral species, it is highly desirable to simplify the complicated spectra associated with all but the simplest species, by use of the supersonic expansion. For clusters, the expansion is also of great utility in simply forming the species for study. Due to the space charge effect, low ionization efficiency by electron impact and high rates of destruction of ions by recombination etc., the number of ionic clusters of a given mass that can be produced from conventional cluster sources is orders of magnitude lower than what can easily be obtained for neutral clusters. Any technique for spectroscopy of charged clusters must take the low density into account.

Although the problem of low number density for ionic clusters makes direct absorption spectroscopy difficult, studies have been made for a few systems. The landmark studies of $H_3O^+(H_2O)_m$ (m=3-5) in 1977[38] and $NH_4^+(NH_3)_n$ (n=2-4) in 1980[39] by Schwarz represent the only gas phase direct absorption spectroscopic measurements of the n,m≥1 species. Schwarz obtained direct infrared absorption spectra by pulse radiolysis of a gas cell containing argon and small amounts of H_2O or NH_3. He made use of the known equilibrium constants for the clustering reactions to deconvolute the absorption signal obtained as a function of pressure into that of the individual cluster ions. The experiments suffered from limited spectral resolution (40 cm^{-1} full-width-half-maximum (FWHM)), relatively high vibrational and rotational temperatures (>300 K), and some ambiguity regarding the distribution of cluster sizes in the sample. Nevertheless, Schwarz was able to observe the ν_3 and $2\nu_4$ vibrational bands of the n=4 ammonium ion core, and to show that the n=3 spectrum was consistent with C_{3v} symmetry. Through isotope substitution measurements, he was also able to establish that the symmetry of the n=4 ammoniated ammonium ion was tetrahedral. For the hydrated hydronium ions, he concluded that the first solvent shell fills at m=3, and observed bands associated with both primary and secondary solvent shells, as well as with the H_3O^+ core.

Direct absorption methods have generated much more information regarding strongly bound molecular ions than for ionic clusters. The technique of velocity modulation detection, developed in

1983, is an extremely efficient means to detect infrared spectra of molecular ions formed in a glow discharge.[37] By means of a bipolar symmetric oscillating electric field between anode and cathode, ions acquire an oscillating drift velocity in the field which is approximately equal in magnitude to their thermal velocity. Due to the Doppler effect, infrared laser spectroscopy of these ions is then equivalent to frequency modulation of the laser in the ion frame of reference. Because the neutrals, to a very good approximation, are not modulated, the use of velocity modulation greatly simplifies the infrared absorption spectrum of the discharge. The resulting spectra are still very complex when many ionic species are present in abundance. Such is the case, for example, in discharges containing carbon and hydrogen. Large amounts of CH_3^+, $C_2H_2^+$ and $C_2H_3^+$ have been found to be present under various conditions, with the probable presence of other species such as CH_5^+ and heavier ions containing more than two carbon atoms.[40] The analysis of the resulting spectrum was difficult and time consuming, since the spectrum of $C_2H_3^+$ is unusual and the carrier of any of the hundreds of spectral transitions could be CH_3^+, $C_2H_2^+$, $C_2H_3^+$ or some other species. The carrier of each transition therefore had to be assigned on the basis of factors such as chemistry, linewidth, and spectral patterns involving the frequency of the transition in question relative to all others. While these methods eventually led to assignments of quantum numbers as well as carrier for many of the spectral transitions in this particular case, an experimental technique which readily discloses the carrier of any given spectroscopic transition is obviously of great utility.

One nontraditional method which nonetheless retains the traditional feature of direct absorption spectroscopy is intracavity laser absorption spectroscopy (ICLAS) of fast ion beams. Infrared spectra of species such as NH_4^+ and HN_2^+ have been obtained with very high resolution because of the kinematic compression of the infrared Doppler profile in the fast beam.[41] In order to obtain sufficient ion beam current for direct absorption studies, the technique uses a discharge followed by expansion with a low backing pressure (10 torr is typical) through a large orifice (1 or 2 mm diameter) with several kV/cm extraction voltage to generate μamps of ion beam current. Under these conditions, the ions can be quite hot vibrationally, since they are accelerated before entering the collisionless regime. Due to the high internal temperature and large partition functions, it is still an open question whether the method can be successfully applied to ionic clusters.

The more successful attempts to gain spectroscopic information about ionic clusters have made use of "consequence" techniques rather than direct absorption methods. Consequence techniques use a direct consequence of photon absorption rather than attenuation of the incident radiation as the signal that an absorption event has taken place. Such methods include, among

others, photodetachment, fluorescence and vibrational predissociation spectroscopies.

5.4.3 Consequence Spectroscopy of Charged Clusters

Consequence spectra of ionic clusters are relatively few in number. Negative cluster ion photodetachment studies have been used to probe the solvated electron.[42,43,44] Inert gas clusters of $C_6F_6^+$ have been studied with laser induced fluorescence and time-of-flight mass spectroscopy to determine solvation effects.[45] Photodissociation studies of various species with intense visible or UV lasers are quite numerous.[46] Picosecond experiments have recently been performed on mass-selected gas phase cluster species,[47] giving the proton transfer rate between cluster subunits after the excitation of one subunit.

Vibrational predissociation techniques have generated the most detailed information so far on hydrogen bonded ionic cluster systems. The first spectroscopic data for the hydrogen cluster ions $H_3^+(H_2)_n$ in any wavelenth region was obtained by such means as well.[48] Other studies of the smaller hydrated hydronium ions (m=1-3) were made, that were able to resolve rotational structure. From these data, and hydrogen "messenger" studies, it was established that the structure of the smallest hydrated hydronium ion ($H_5O_2^+$) is symmetric with respect to the position of the proton between the two waters.[49,50] This data is valuable in that it provides information relevant to the analysis of the proton transfer potential.

Recently, Lisy and coworkers have studied $Cs^+(CH_3OH)_n$ (n=4-25) clusters with an apparatus similar to the apparatus to be discussed in detail in the next sections.[51] A line-tunable CO_2 laser produces enough vibrational predissociation to observe depletion of a mass-selected cluster ion beam. It has been concluded from the spectral data that the first solvation shell about the cesium ion consists of ten methanol molecules, and that larger species are composed of small hydrogen bonded clusters of methanol bound to the surface of the solvated ion. Monte Carlo simulations with pairwise potentials were found to be consistent with these interpretations. They have studied the $Na^+(CH_3OH)_n$ system very recently.

5.4.4 Basic Principles of the Experiment.

Our work makes use of a vibrational predissociation technique involving a mass selected ion beam and a radio frequency (RF) ion trap. The experimental apparatus is shown schematically in Figure 1. We shall refer to it, at times, as a MAMICS or Mass Analzed Molecular Ion Consequence Spectroscopy apparatus. The principle elements are an ion source which incorporates a supersonic expansion, two stages of mass selection (a magnetic

mass spectrometer and a quadrupole mass filter), an octupole ion trap and an infrared laser source. Several of the important components of the device will be discussed in detail below, but a brief overview is in order.

Cluster ions are generated by one of a number of sources. Of the distribution of cluster ions created by the source, one is selected for study by means of a sector-type mass analyzer. The mass selected beam is then directed into a radio frequency ion trap which holds the cluster ions of interest under collision free conditions while they interact with a tunable infrared laser. If sufficient energy is absorbed from the laser through the excitation of one of the high frequency stretching motions of the ion core or the solvent molecules, the weakly bound clusters may undergo vibrational predissociation along a channel involving the loss of one or more solvent molecules.

After excitation, the contents of the trap are then directed into a second mass spectrometer tuned to pass fragment ions of a particular mass. Since the appearance of the mass selected daughter ions is a direct result (or consequence) of the absorption of one of the tunable infrared photons by the larger parent cluster ions, these smaller massed product ions can be used as a signal that an absorption has taken place. Plotting the number of daughter ions produced as a function of the tunable infrared wavelength yields, to a first approximation, the absorption spectrum of the parent ion. More details of the excitation scheme and the approximations involved in this technique are given below.

In contrast to direct absorption methods, the sensitivity of this technique is extremely high. Ion counting permits the detection of single absorption events with essentially zero background at the mass of interest. For typical conditions in the experiments described below, we have an infrared absorption cross section $\sigma \approx 10^{-17}$ cm^2, an absorption pathlength $l \approx 100$ cm, and an ion beam density $n \approx 10^3$/cm^3. The fractional absorption, given by $n\sigma l$, is then on the order of 10^{-12}, at least five orders of magnitude more sensitive than the detection limit of the best direct absorption experiments.[52]

5.4.4.1 Ion Sources

Among the sources which could be used for generating hydrogen bonded cluster ions are a) the Lineburger source[53], b) the duoplasmatron[54], c) the corona discharge[55], d) the electrospray ionization source (ESI), e) impact of high energy particles such as protons, f) ionizing radiation from radioactive isotopes, and g) electron impact ionization of neutral clusters. Each of these have advantages and disadvantages.

The ion density associated with f is normally low. The ESI source shows great promise but is not well characterized. Sources b and d can produce large numbers of ions, but these are internally hot. Method e requires a source of high energy particles, which is usually unavailable. Like b and g, e also tends to produce large numbers of ions, but these are again internally hot. However, if the ions are made to drift through a region containing a buffer gas at high pressure and expanded through a nozzle, they can be made internally quite cold.

The corona discharge followed by a supersonic expansion is the source used in these experiments and appears in Figure 2. It is able to produce internally cold ionic clusters at a medium flux level, and therefore represents a good compromise. Our typical conditions for the operation of the corona discharge involve tens of microamps of discharge current and very low extraction voltages (<5V) between the 70 μm source nozzle and the skimmer to the second differential region of the machine. The low voltage difference is used to prevent the ions from accelerating into the neutrals during the supersonic expansion between the nozzle and the skimmer, resulting in vibrational heating of the ions and possible dissociation of the clusters. To further improve cooling, the source may be kept in thermal contact with a liquified gas reservoir. Ion flux is low under these conditions (on the order of 10^7 ions/sec summed over all masses) but the internal temperature of the clusters is also low (less than 30 K rotational temperature and substantially below room temperature vibrationally).

The ion flux can be increased by enlarging the nozzle diameter and/or increasing the extraction voltage (the voltage difference between nozzle and skimmer). The price paid for this is higher internal temperature and a shift in ion abundance distribution toward the smaller clusters. With a nozzle diameter of 1 mm or larger, extraction voltage of several kV and a low pressure, high current discharge, ion currents of 10 μA can be obtained as mentioned in section **5.4.2**, instead of the pA levels of the current experiments. With such large currents, direct absorption spectroscopy of some of the species in an ion beam could be possible.

5.4.4.2 Mass Selection and Ion Storage

The distribution of clusters produced by the corona discharge source is directed onto the entrance slits of a 60-degree sector type mass spectrometer with a mass resolution of $m/\Delta m = 150$ (see Figure 2). This level of resolution is routinely achieved by the experimental apparatus, but relies strongly upon the monochromaticity of the ion beam. Variations in the energy of the ions must be minimized, and to some extent, the resolution is dependent upon the conditions of the ion source. Large voltage differences between the nozzle of the source and the skimmer

shown in Figure 1 lead to degradation of the mass resolution due to fringing field effects.

Following the mass selection, ions of the desired mass are deflected 90° by a dc quadrupole bending field, decelerated and focused into the octupole ion guide whose axis is that of the infrared laser beam. The octupole consists of eight molybdenum rods, equally spaced on a 1.5 cm radius. The rods of the octupole carry approximately 350 volts dc, with applied radio frequency voltages of typically 300 volts peak to peak. Adjacent rods are maintained 180° out of phase. The capacitance of the rods together with the inductance of a copper coil atop the machine form an LC tank circuit which is made resonant in the range 5-20 MHz by the choice of the coil. Smaller ions such as H_5^+ are trapped most efficiently at frequencies toward the high end of the range.

Trapping is accomplished by means of entrance and exit repellers, each of which carries a positive ≈ 350 volts dc. Upon these a negative 12 volt pulse may be applied to allow the entrance and exit, respectively, of ions into and out of the octupole. The relative timing is adjustable to vary the storage time and the ions can be easily stored for $t < 1$ minute with only about 50% losses. The upper limit to our trapping time is determined by the $\approx 10^{-9}$ torr background pressure in the UHV region of the octupole. The number of trapped ions is optimized by adjusting the dc voltage on the rods: the dependence is rather sharp. One thousand ions are routinely trapped at a time, with a repeat frequency of 40 Hz. The major limitation in the number of stored ions seems to be the low ion flux from the source. The trapped ion energy in the longitudinal direction is < 0.5 eV.

The choice of an octupole ion trap over the simpler quadrupole design stems from the superior shape of the effective potential that an octupole field generates. For the present case of a fast oscillating field, the effective potential governing the motion of a slow moving particle with charge q in an ideal electric multipole field with 2n poles is given by:

$$U_{eff}(r) = n^2 K \left(\frac{r}{r_0}\right)^{2n-2} \qquad (1)$$

where K is described by:

$$K = \frac{q^2 V_0^2}{4m\omega^2 r_0^2} \qquad (2)$$

and V_o is the rms rf voltage, r_o is the trap radius, ω is the rf angular frequency and m is the mass of the particle. For an octupole, the effective potential varies as $(r/r_0)^6$.[56] This dependence is $(r/r_0)^2$ for a quadrupole, with a well depth only 25% of the octupole depth for a given voltage, mass, and frequency.

5.4.4.3 Laser Excitation and Consequence Detection

The trapped, mass-selected ionic clusters are vibrationally excited by a pulsed infrared laser derived from the difference frequency mixing, in a $LiNbO_3$ crystal (Quanta Ray IR WEX), of a Nd:YAG laser fundamental (1064 nm) and tunable dye laser radiation (typically 740-835 nm). With the aid of a feedback loop, this commercial unit automatically adjusts the tilt of the crystal to maintain the phase matched condition for difference frequency generation as the dye laser is scanned. Typical laser power is 3.5 mj/pulse at 4000 cm^{-1}.

For neutral clusters or weakly bound ionic clusters such as the hydrogen cluster ions (see Table I), a single photon of tunable infrared light in the 4000 cm^{-1} region provides sufficient energy to promote the system over the dissociation threshold along the solvent molecule loss channel. Absorption of a photon into one of the high frequency stretching modes of the ion core in $H_3^+(H_2)_3$ results in the loss of up to two of the three available H_2 ligands.[57] For weakly bound systems, excitation of a single quanta of a high frequency vibrational stretch can couple to the continuum of levels of the dissociating products.

For weakly bound systems like these, the absorption spectrum of the parent cluster ion should be well represented by the number of daughter ions produced as a function of the tunable infrared light. The frequency dependence of the reaction cross section for the photodissociation reaction

$$H_3^+(H_2)_n + h\nu_1 \rightarrow H_3^+(H_2)_{n-1..2} + (1..2)H_2 \qquad (3)$$

comes only from the frequency dependence of the absorption cross section of the parent cluster.

The situation becomes somewhat more complicated when the ionic cluster in question has a binding energy larger than the energy of a single tunable infrared photon. Under these circumstances, more energy must be deposited in the system to induce dissociation unless there are large amounts of internal excitation already present. Virtually all of the systems studied in this work fall under this category. A glance at Table I reveals that for the hydrated hydronium or ammoniated ammonium ion dimer species (either a hydronium or an ammonium ion solvated by a single ligand) the ΔH° of formation is roughly a factor of three larger than the energy of a 3000 cm^{-1} photon. Only for the

largest clusters is the binding energy small enough for a single photon to be effective in removing a solvent molecule. To put the required extra energy into the system we have turned to a multiphoton excitation scheme.

For all but the largest clusters in this study, a second laser is also used. Once the cluster has absorbed a tunable infrared photon, it is in an energy regime characterized by a very high density of states referred to as the quasi-continuum. Stepwise excitation of the cluster in this region by a line tunable CO_2 laser (MBP Technologies, 8 Watts cw at 10.6 μm) is a reasonably facile process, and through this stepwise excitation the cluster can obtain sufficient energy to undergo loss of one or more solvent molecules. This reaction is represented in its most general form for positive ionic clusters by the following:

$$A^+(M)_n + (h\nu_1) + m(h\nu_2) \rightarrow A^+(M)_{n-i} + iM \quad (4)$$

In this case, $(h\upsilon_1)$ represents a tunable infrared photon of frequency υ_1 and $m(h\upsilon_2)$ represents m number of fixed frequency photons of frequency υ_2. The parent cluster in this case has absorbed sufficient energy from the two lasers to result in the evaporation of i solvent molecules to produce a smaller massed daughter ion.

Since the spacing between energy levels is much larger in the low energy regimes, the absorption cross section for the tunable infrared photons is large only at a strong resonance with a fundamental vibrational transition. The total cross section for the photodissociation reaction above is assumed to have wavelength dependence only from the absorption cross section for the first tunable infrared photon which excites low lying vibrational states. Daughter ions are counted using a Daly ion detector, and spectra are usually normalized for the tunable infrared power using a simple linear power dependence.

5.4.5 Typical Results and Interpretations

Presented below are representative data obtained using the MAMICS technique for a number of ammoniated ammonium ions $(NH_4^+(NH_3)_n)$, hydrated hydronium ions $(H_3O^+(H_2O)_m)$, and an example of a cluster involving both ammonia and water around an ammonium core $(NH_4^+(NH_3)_3(H_2O))$. While the MAMICS apparatus can be adapted to study high frequency stretching overtones or electronic spectra below 2.5 μm, the data to be discussed here pertain only to the 2.5-4.0 μm region of the spectrum. The spectral features which appear here are due primarily to vibrational fundamentals involving the high frequency NH or OH stretches of the solvent molecules and the ion cores of the clusters. Other, weaker features have been assigned to bending overtones or combination bands involving bends and NH or OH stretches.

thought to have an ammonia in the second solvation shell. We have assigned this feature to components of the N-H stretching modes of the core where the N-H bonds are involved in hydrogen bonding to both 1° and 2° NH_3's.

Between the B and E series lies the bending overtone $2\nu_4$ of NH_3 ligands and the N-H oscillator of 1° NH_3 which is hydrogen bonded to 2° NH_3. There is little doubt that the latter contribution accounts for much of the substantial increase in relative intensity of series D from n=5 to n=8. The series E also arises from N-H oscillators of 1° NH_3 and increases considerably in intensity relative to the most intense band for a given n, from n=5 to n=8. For E, it is much more obvious that the first appearance is at n=5. The series is due to the two equivalent N-H oscillators of 1° NH_3 with a 2° NH_3 hydrogen bonded to its remaining N-H. Series D and E correspond in some measure then to symmetric and antisymmetric stretching modes of 1° NH_3 with attached 2° NH_3. As such, there is some possibility of Fermi-resonance interaction between the modes. Such an interaction may account for the negative $\Delta\nu/\Delta n$ of series D. Even so, D and E have their smallest $|\Delta\nu/\Delta n|$ values at large n, like the other series.

Between D and E, weaker features appear, tentatively assigned to the symmetric stretch of the three equivalent N-H oscillators of 2° or 1° NH_3 and/or symmetric stretches of the two equivalent bonds of 1° NH_3 with 2° NH_3 attached to the third oscillator. The rather intense feature centered at $\approx$ 3370 cm^{-1} in Figure 4a is due to the single N-H oscillator stretch of the n=3 NH_4^+ core, where the H is <u>not</u> hydrogen bonded to a 1° NH_3.

The most striking feature of the spectra between 2600 and 3500 cm^{-1} is a weak band originating at roughly 3400 cm^{-1} composed of a number of resolved subbands having a separation between adjacent components of about 12 cm^{-1}. Shown in Figure 5 for n=1 to 6, this spacing is about twice the rotational constant for NH_3 about its C_3 symmetry axis. We have been able to show that this structure arises from a vibrational transition of the solvent molecules in the first solvation shell involved in a nearly free rotation about the hydrogen bond to the ion core. The vibration is analogous to the doubly degenerate antisymmetric stretch, υ_3, of free ammonia, which occurs at 3444 cm^{-1} in the gas phase[61] (see figure 3).

Such a vibrational band carries the selection rule $\Delta K=\pm1$, where K is the quantum number for angular momentum about the NH_3 C_3 axis. The assignments of the internal rotation subbands are given in Figure 5 and the notation is that used for a perpendicular vibration-rotation transition of a strongly prolate symmetric top molecule. While this notation is not strictly correct for the case of internal rotation, we use it for convenience as it follows easily from the picture of an ammonia molecule attached

to a "wall" along its C_3 axis. Such structure cannot be expected for any vibrational band of the core or any solvent vibrational band, such as the symmetric stretch ν_1 of NH_3, which carries a $\Delta K=0$ selection rule. The fact that the structure is observed for n=5 and 6 indicates that some first shell solvent molecules can still be quite unhindered even when the second solvation shell has begun to be filled. Further discussion of internal rotation within ionic clusters can be found in later sections.

5.4.5.2 $H_3O^+(H_2O)_m$, m=3 to 8:

Recently, we have extended our early studies of the hydrated hydronium ions to the larger cluster ions where m is greater than 3 and the second solvation shell is formed.[62] Figure 7 contains the spectra of m=3-8 in the 2600-4000 cm^{-1} region (with the exception of m=7 and 8 where only the region 3200-4000 cm^{-1} was obtained). It is instructive to compare some of the general features of these data, and the data for the ammoniated ammonium ions discussed above. The spectra of $H_3O^+(H_2O)_m$ are similar to those of $NH_4^+(NH_3)_n$ in several respects, including a) the presence of band series decreasing in $\Delta\nu/\Delta n$ as n increases, b) a clear separation between those bands associated with non-bonded oscillators, 1° or 2° ligand bonded oscillators, and hydrogen bonded oscillators of the ion core, and c) agreement with the rough empirical correlation of width and frequency of the bands with the strength of the hydrogen bond.[18]

Previously, theorists and experimentalists collaborated heavily to determine that $H_5O_2^+$ (n=1) has a single minimum potential with respect to the proton involved in the hydrogen bond. The minimum energy position was found to be midway between the oxygen atoms. The Schaefer group has calculated geometries, vibrational frequencies and intensities for $H_3O^+(H_2O)_m$ ($m\leq3$) using full configuration-interaction with single and double excitations in the simulation. These are the highest level <u>ab initio</u> calculations yet performed for ionic clusters.

For larger systems, due to the expense of the Schaefer-type calculations, other methods have been used such as Monte Carlo (MC) and Molecular Dynamics (MD) simulations. These methods assume that the summation of pairwise interaction potentials between molecular groups will give an accurate description of the potential energy surface. The MC method has given predictions concerning the structure and thermodynamic properties of solvated ions in solution and in the gas phase.[63,64,65] For example, Kochanski has predicted that the presence of four water molecules in the first solvent shell has a significant probability in the $H_3O^+(H_2O)_m$ species if m is considerably larger than 4, and that successive shells will tend to begin filling before the previous one is full.[63] When the pairwise potentials are well known, the results tend to be reliable. Recent MD simulations have been conducted on ion-water systems.[66,67]

The m=3 spectrum (figure 7a) is the only one in this set of data for which vibrational frequencies have been calculated at a high level of theory. The vibrational transition of the H_3O^+ core with the largest predicted intensity is the antisymmetric stretch of the three O-H oscillators. The ab initio frequency for this mode was 2997 cm^{-1} for a C_{3v} structure, with the symmetric stretch 23 cm^{-1} higher and a factor of 40 less intense.[68] The experimental spectra from Schwarz's previous direct absorption measurements and our own consequence technique show a rather broad band centered at 2670 cm^{-1} and a weaker one at 3050 cm^{-1}. Schwarz assigned the 2670 cm^{-1} feature to the core antisymmetric stretch. This feature and its analogous counterparts in the spectra of the larger clusters is designated by series A of Figure 7. If this assignment is correct (the antisymmetric stretch band is expected to be the most intense feature of the spectrum below 3000 cm^{-1}, which this band is), it means that the theoretical calculation is wrong by more than 300 cm^{-1} for the frequency of this vibration, or more than 10%. The usual accuracy for small, polyatomic molecules is better than 2 or 3%. The poor accuracy for the cluster systems results from an inadequate treatment of the effect of hydrogen bonding. One obvious difficulty is that the most sophisticated calculations still do not consider the influence of anharmonicity directly, and instead apply a semi-empirical scaling factor to a calculated harmonic frequency. The scaling factor is often taken to be the same for all modes.

The symmetric stretch of the m=3 core has been a source of some controversy, especially since Schwarz and Newton[69] identified it with the weak band at $\approx$ 3000 cm^{-1} but the recent ab initio calculation placed it only 23 cm^{-1} above the antisymmetric stretch.[68] We believe the 3050 cm^{-1} band to be the same feature Schwarz observed, but assign it to either a bending overtone, most probably of the solvent molecules, or a combination band which would likely involve the core antisymmetric stretch and a hydrogen bond stretching vibration (the harmonic frequency of the antisymmetric stretch involving $\nu_{O\cdot H\text{-}O}$ in the m=3 C_{3v} structure is of the order of 300 cm^{-1},[68]). In figure 7b, the band of series A has a less intense companion about 70 cm^{-1} to the blue; this is probably the core symmetric stretch. For a structure of type similar to the ammoniated ammonium case but with 3 instead of 4 solvent molecules in the first and second shells, series A should consist of a single band for m=5 (it does), probably with significantly reduced intensity since stretches of the core will only carry high intensity for antisymmetric stretches of two or more equivalent oscillators. Indeed, the intensity is low, as it was for the analogous band of n=7 ammoniated ammonium.

Series B, which begins at m=4, and seems to continue through m=8, can be identified quite readily with the stretch of O-H oscillators of 1° H_2O which are hydrogen bonded to 2° H_2O. The width of the m=4 peak seems a bit large compared to the rest of

the series, and might arise from an overlapping band on the low frequency side; m=5 also has a broad feature in this region. A comparison of m=5 with m=4 and 6, however, after mentally removing the presence of series B, suggests that the m=5 spectrum might be anomalous. It has broad absorption in the 3150 - 3450 cm^{-1} region which appears similar to the m=4 spectrum if the series A band of m=4 is included, but bears little resemblance to the m=6 case with or without the series A band. One possible explanation is the presence of a second isomer of m=5.

According to Newton, a structure for the m=5 ion involving an $H_5O_2^+$ ion core should exist.[70] Designated $H_5O_2^+(H_2O)_4$, this species should have a global minimum energy only 2.5 kcal/mole above that of the $H_3O^+(H_2O)_5$ structure. Newton proposed this structure to be an important intermediate in the proton transfer mechanism in aqueous acid solution, with the symmetry of the $H_5O_2^+(H_2O)_4$ complex being essential to the mechanism. The expected stretching frequencies of the four equivalent O-H oscillators in the $H_5O_2^+$ core are, of course, unknown, but should certainly fall somewhere between 3000 and 3400 cm^{-1} and carry a large intensity. The low relative intensity of the series B band in the m=5 spectrum, compared to the trend of m=4-8, may offer some small support for the $H_5O_2^+(H_2O)_4$ hypothesis. If the hypothesis is correct, a very intense, very broad band should exist somewhere in the 500-2000 cm^{-1} region, arising from the vibration of the central $H_5O_2^+$ proton.

Series C and E arise, respectively, from the symmetric and antisymmetric stretching modes of the ligands which have none of their O-H bonds involved in a hydrogen bond. As solvent molecules with all O-H oscillators free, the O-H stretching frequencies are shifted very little from their isolated gas phase values. In n=5, for example, the shifts are $\approx$ 4 and $\approx$ 15 cm^{-1} to the red for symmetric and antisymmetric stretch, respectively (see table IIb). Because of the small shifts, contributions from ligands in more than one shell tend to overlap. The decreasing relative intensity from m=3-8 suggests, however, that the absorption cross section decreases in the order 1°>2°>3° for these oscillator types.

The assignment of a given spectral feature is made primarily on the basis of the lowest solvation number for which it is present, the frequency at which it appears, and the change in relative intensity with solvation number. Series D begins as the second solvation shell begins to form with the m=4 cluster and increases in relative intensity as a function of cluster size to dominate the spectrum by m=6. We have assigned this feature to the free O-H stretch of an H_2O that has one of its O-H oscillators involved in a hydrogen bond with another solvent molecule. Since molecular species tend to carry a transition dipole moment which increases with partial charge, a general trend with respect to absorption cross section of core>1° is expected when similar

oscillators are compared. Theoretical calculations show that the partial charge decreases in the order core>1°>2° so we would expect that most of the intensity associated with this peak is due to transitions involving the H_2O's in the 1° shell bound by 2° H_2O's.

A similar series begins very weakly at m=6 and is very apparent at m=7, where the third solvation shell is expected to begin filling. This feature is attributed to the free O-H stretch of species involved in hydrogen bonding to <u>both</u> 2° and 3° H_2O's. It is labeled F in the figure. If this assignment is correct it confirms the Monte Carlo prediction mentioned above, that the higher solvation shells may begin to fill before the lower shells have been completely occupied.

While the vibrational predissociation spectra of $NH_4^+(NH_3)_n$ become somewhat indifferent to an increase in n above n=7, the spectra of $H_3O^+(H_2O)_m$ evolve considerably from m=6 to 7 and 7 to 8, in spite of the fact that each shell is thought to contain only three ligands instead of four. This can be attributed to at least two factors: 1) the larger intrinsic hydrogen bonding interaction of H_2O as compared to NH_3, and 2) a larger absorption cross section for H_2O than for NH_3 in the secondary and tertiary solvation shells. Even the spectrum of the gas phase cluster $(H_2O)_{17}$ is known to have a sharp feature at about 3710 cm^{-1},[71] corresponding to the non-bonded O-H stretch of H_2O ligands where the other O-H is part of the hydrogen bonded network. The $(H_2O)_{17}$ spectrum is more reminiscent of liquid water in the 3100-3600 cm^{-1} region, however, which consists of a very broad, featureless absorption. It is not really difficult to imagine that the spectrum even of $H_3O^+(H_2O)_{17}$ is similar in this region.

The spectrum by m=8 has several broad peaks, arising from various hydrogen bonded O-H oscillator stretching vibrations. These could include 1° O-H to 2° H_2O, 1° O-H to 2° H_2O to 3° H_2O, and 2° O-H to 3° H_2O. Bending overtones may appear in the 3100-3300 cm^{-1} region as well. As the cluster size grows, the number of possible types of hydrogen bonds increases further, with a resultant filling effect in the 3100-3500 cm^{-1} spectral region. Further, the ratio of hydrogen bonded to free O-H oscillators is certain to rise, with a resultant decrease in the relative intensity contribution of free O-H oscillators in the 3600-3800 cm^{-1} region. The difference between spectra of hydrated hydronium and neutral water clusters should become small when the size of the clusters is very large (hundreds or thousands of H_2O subunits). For the intermediate case, vibrations of the ion core and the inner shell(s) account for most of the difference.

5.4.5.3 $NH_4^+(NH_3)_3H_2O$

In addition to studying the proton solvated by just one type of solvent molecule, we have investigated the spectra of a number of "mixed" cluster species containing both NH_3 and H_2O.[72] These species are of particular interest, as they provide information about chemically heterogeneous systems and perhaps can shed some light upon the sorts of solvent-solvent interactions encountered in bulk mixtures. We present here the spectrum of $NH_4^+(NH_3)_3H_2O$ (see figure 8) over the frequency range of 2600-4000 cm^{-1}, which serves to illustrate many of the essential features observed.

When a hydrated hydronium species $H_3O^+(H_2O)_m$ encounters NH_3, a proton transfer reaction is likely to take place resulting in the formation of the species $NH_4^+(H_2O)_{m+1}$. Since the proton affinity of H_2O is 6.5 eV vs. 8.9 eV for NH_3,[73] the energy released by the process is in the neighborhood of 2 eV, or about 40 kcal/mole. In our experiment, this excess energy is removed through collisions in the supersonic expansion or through the evaporation of solvent molecules from the cluster. The strong favoring of the proton transfer reaction to the ammonium side leads us to assign all mixed cluster peaks in our mass spectra to the isomers containing an ammonium rather than a hydronium core.

Competition occurs between the heterogenous solvent molecules for sites around the ammonium ion during the cluster's formation. A number of experiments have been made studying the $\Delta H°$ of formation for the stepwise solvation of the ammonium ion by both water and ammonia. Some of these results appear in Table I. It has been shown that the hydrogen bond of $NH_4^+(NH_3)$ is much stronger than that of $NH_4^+(H_2O)$.[74] The affinity of NH_3 for $NH_4^+(NH_3)_n$ is higher than that of H_2O for $NH_4^+(H_2O)_n$ in the first solvation shell ($n \leq 4$) because of the greater proton affinity of NH_3. The difference decreases with increasing n however, and is nearly zero for n=4, which represents a crossing point. In the second solvation shell, additional H_2O's bind more strongly to the $NH_4^+(H_2O)_n$ than NH_3's do to $NH_4^+(NH_3)_n$. This is because the hydrogens involved in second shell hydrogen bonding are more similar to the hydrogen atom than a proton since the charge has been delocalized over the entire cluster; the hydrogen bonding interaction of H_2O with neutral H_2O or NH_3 is stronger than that of NH_3. The $NH_4^+(NH_3)_3H_2O$ cluster is particularly interesting as one of the systems where ammonia and water are held with nearly the same energy.

The spectrum of the n=3,m=1 cluster appears in figure 8 over the frequency range of 2600 to 4000 cm^{-1}. Over the spectrum are shown three isomers which we consider sigificant to our discussion. Structure I has the three ammonia molecules oriented about the ammonium ion with their C_3 axes along the axes of the N-H bonds of the core. In this case, the water molecule is oriented along its C_2 symmetry axis. This orientation is

stabilized by a favorable ion-dipole interaction involving the N-H bond and the dipole moment of the H_2O. In structure II, the water molecule is still attached to the ion core, but one of the ammonia molecules has adopted a 2° solvation site, and has attached itself to the water. Structure III shows the opposite configuration, where the water has adopted the 2° solvation site and attaches itself to one of the 1° ammonia molecules.

A variation on isomer I merits some discussion. It could happen that the water molecule binds to the ammonium ion oriented along an orbital containing a lone pair of electrons. In this case the water molecule would be substantially tilted from the orientation shown in the figure. A tilted orientation of H_2O is observed, for example, in the hydrogen bonding of ice and in HF-H_2O.[75]

As in the case of the ions studied previously, features are observed that can be assigned to transitions arising from the vibrational motions of both the solvent molecules and the ion core of the cluster. It is evident from figure 8 that nearly free internal rotation of NH_3 occurs in the $NH_4^+(NH_3)_3H_2O$ complex, as the same structure (labeled C in the figure) observed for $NH_4^+(NH_3)_n$ (n=1-6) is present in the 3400 cm^{-1} region. The frequency of the "^RQ_o" subband of the NH_3 ν_3 fundamental is identical for $NH_4^+(NH_3)_3H_2O$ and $NH_4^+(NH_3)_4$ (Figures 5d,4b) to within 2 cm^{-1}. In the higher frequency region, structures are present which obviously correlate to the symmetric (labeled D) and antisymmetric (labeled F) stretches of the solvent molecules in the $H_3O^+(H_2O)_m$ (m=1 to 8) systems. The strong features between 2600 and 3200 cm^{-1}, (labeled A) have been assigned to modes of the ion core. While the spectrum is similar in areas to both the hydrated hydronium and the ammoniated ammonium spectra there are significant differences as well.

In the case of $NH_4^+(NH_3)_4$, the evidence is strong that the local C_3 axis of each NH_3 coincides with an N-H bond axis of NH_4^+. The evidence includes Schwarz's determination of a tetrahedral equilibrium structure, the very low barrier to internal rotation of NH_3, the relative intensities of the NH_3 ν_3 subbands, and the numerical value of the characteristic subband spacing. In the spectrum of fig. 8 (x=3,y=1 spectrum), structure I is clearly present as a constituent. We see three narrow peaks (F in the figure) with $\approx$ 29 cm^{-1} separation, in the 3700-3800 cm^{-1} region where the ν_3 antisymmetric stretch of H_2O is expected. If this structure is due to the same sort of internal rotation seen for NH_3 in the ammoniated ammonium ions, the separation observed should be roughly twice the constant for rotation about the internal rotation axis. Indeed, the constant for rotation about the local C_2 axis of H_2O is 14.5 or 29/2 cm^{-1}.

As was the case for internal rotation in the ammoniated ammonium ions, only a perpendicular band of the solvent H_2O can show such internal rotation structure. The spin weight with respect to the

quantum number K (once again, we are adopting a much simplified picture of the complex, essentially H_2O attached to a wall) for the angular momentum about the H_2O C_2 axis, by analogy with formaldehyde-type molecules, is 1 for K=even and 3 for K=odd. As a result, $^RQ_0$ is less intense than $^RQ_1$ or $^PQ_1$, in spite of the Boltzmann factor which, for kT=25 cm^{-1}, is $I(K=1)/I(K=0) \approx \exp(-14.5/25) = 0.56$ (while $^PQ_1$ has a greater peak height than $^RQ_1$, the integrated intensities appear to be comparable). This internal rotation structure could not be observed from isomer II, as the 2° ammonia would quench the free internal rotation of the water. Isomer III is also unlikely to produce this structure, particularly in view of the observation that only first shell subunits in ammoniated ammonium complexes seem to give rise to a nearly free internal rotation band structure.

The sharp band labeled B is not present in the n=4 ammoniated ammonium cluster, but is observed for the n=3 ammoniated ammonium ion. There, it was assigned to a core stretching band primarily associated with the single free N-H oscillator of the core. It appears in the spectrum of the n=3,m=1 cluster with nearly the same frequency and intensity relative to the ammonia internal rotation structure. This points to isomers of type II or III being present, where one of the sites on the ammonium ion is free, resulting in one high frequency core N-H stretching band. The presence of a sharp, strong band at about 3380 cm^{-1} is a signature of this vibrational mode, since the frequency will not depend strongly upon the solvation of the other 3 binding sites.

Recall that in the section on the hydrated hydronium ions, a high frequency feature was observed in the m=4 spectrum correlated with the addition of a solvent molecule into the second shell. Labeled D in Figure 7b, it was assigned to the free O-H stretch of a 1° water bound by a 2° water. This band also provides a signature, since it must appear quite close to the average of symmetric and antisymmetric stretching frequencies of an H_2O at that binding site. Isomer II of the n=3,m=1 mixed cluster should show a similar, free O-H stretch. The peak at 3710 cm^{-1} labeled E in figure 8 has been assigned to this. Isomer I is clearly more stable than isomer II, from the observation that if the gas pressure behind the expansion nozzle is increased to lower the cluster ion internal temperature, a significant intensity reduction of peak E relative to peaks F takes place.
Given the greater competitiveness of NH_3 for the inner solvent shell and H_2O for the outer solvent shell from the thermodynamic measurements cited above, one might predict an isomer with 2° H_2O hydrogen bonded to a 1° NH_3 to be more stable than isomer II. There is no clear evidence in the spectrum for such an isomer, however, nor the variation on isomer I discussed above where the water is tilted, and no clear evidence for isomer III. Another possible isomer involves one free core oscillator, and the H_2O

subunit binding equally to two of the core hydrogens via highly nonlinear hydrogen bonds involving the oxygen lone pairs.

5.4.6 Concluding Remarks

5.4.6.1 Aspects of Internal Rotation:

It was not known whether nearly free internal rotation (barrier height < 20 cm^{-1}) would be observed in the hydrogen bonded ionic cluster species, which are relatively strongly bound cluster systems. The influence of internal rotation tunneling effects has been observed in many of the van der Waals molecules investigated to date, but relatively few species have been found to have barrier heights less than 100 cm^{-1}, especially if we ignore clusters containing rare gas atoms or H_2.[76] NH_3-CO_2 is one of the exceptions which falls into the category of nearly free internal rotors.[77] Internal rotation seems to have been observed in the spectrum of H_5^+; the band at 4250 cm^{-1} must be the v=1,J=2 ← v=0,J=0 transition of the loosely bound H_2 subunit (H_5^+ can be thought of as $H_3^+ \bullet H_2$). Due to the large rotational energy of > 300 cm^{-1} in the upper state, however, the barrier to internal rotation of H_2 in this case could conceivably be 100 cm^{-1} or more - the dependence of such transitions upon the barrier height is not rigorously known. It is likely that the majority of ionic clusters containing loosely bound H_2 will undergo a similar transition. It is interesting to note that the barrier to rotation of H_2 in crystalline (solid) H_2 is on the order of 1 cm^{-1}.[78]

For the smallest clusters, internal rotation of the subgroups can be given the same sort of rigorous theoretical treatment previously applied to analogous neutral molecules. The spectrum of the n=1 ammoniated ammonium ion has been modeled with the same formalism applied to molecules like dimethylacetylene, where the methyl groups rotate relative to each other through a three-fold potential.[58,79] Figure 9 shows the results of this modeling for $NH_4^+(NH_3)$. It was found that in the case of $NH_4^+(NH_3)$ the internal rotation is nearly free (< 10 cm^{-1} barrier height to the motion) and that the spectrum at 1 cm^{-1} resolution is consistent with a symmetric equilibrium structure, although it is not shown conclusively that the symmetric structure corresponds to a potential minimum.

The discussion of hydrated hydronium spectra in section **5.4.5.2** is conspicuous for the absence of any mention of internal rotation. Indeed, the internal rotation barrier for H_2O in hydrated hydronium is clearly much higher than it is in $NH_4^+(NH_3)_3H_2O$ or for ammonia in the $NH_4^+(NH_3)_n$ complexes ($n \leq 7$). On the other hand, the barrier is very likely to be less than several hundred wavenumbers, and there is even a hint in the spectrum that the excitation of a low frequency torsional vibration involving H_2O may result in a greatly increased tunneling rate.[62] The presence of a nonbonding electron pair in

the p_x and p_y orbitals of water may be related to the fact that the 1° NH_3 solvent subunits in the ammoniated ammonium species rotate freely ($n \leq 7$) but the waters in hydrated hydronium do not. Since the H_2O in $NH_4^+(NH_3)_3H_2O$ clearly rotates with a very low barrier, the interaction of a single H_2O subunit with the rest of the ammoniated ammonium complex is not sufficient to create a substantial barrier. When additional NH_3 subunits are replaced by H_2O, however, the features of the H_2O antisymmetric stretching band are broadened considerably. The system with $n + m = 3$ exhibits a very similar phenomenon, although the symmetry of the ion is different. When all three or four subunits are H_2O the broadening is greatest. The broadening and complication of the structure is presumably associated with a more complex potential function and a higher barrier height. It seems to be the case, therefore, that the H_2O subunits interact with each other. This interaction could be primarily through their strong dipole moments, for example, possibly making the hydrogen bonds slightly nonlinear and therefore complicating the internal rotation, or it might be more directly related to the electronic structure as already mentioned. In any case, the barrier even in $NH_4^+(H_2O)_4$ is clearly lower than in $H_3O^+(H_2O)_4$ or the other hydrated hydronium species, indicating that other factors also play a role. One very important factor is the symmetry with respect to the internal rotation. Six-fold barriers are inevitably lower than three-fold or two-fold barriers.[80] In the n=3,m=1 cluster the barrier with respect to H_2O rotation is six-fold, provided that we neglect to consider the hydrogens of the other subunits. For the m=1-3 hydrated hydronium clusters, the analogous barrier is only two-fold, and the higher barrier height is not unexpected. Since the barrier can be either two-fold or three-fold in ammoniated ammonium complexes which exhibit nearly free rotation of 1° NH_3 subunits, both symmetry and subunit interaction are important factors.

5.4.6.2 The Transition from the Gas to the Liquid Phase:

The properties of clusters evolve with size and become similar to those of bulk materials in the limit of very large clusters (see, for example, section VI of this volume). Trends in the measured vibrational frequencies are observed for both core and solvent vibrations in all of the systems investigated in this work. For the ammoniated ammonium ions, these trends are particularly apparent. For the most part, observed features undergo a progressive blue shift as the solvation number, n, increases. This shift is due to the decrease in average hydrogen bond energy for a given bond type as the solvation number is increased. Delocalization of the charge over the cluster is the primary factor which reduces the "per-ligand" interaction strength with the ionic core of the cluster. In the limit of complete dispersal of the charge (large cluster limit), hydrogen bonding energies of successive subunits should approach a constant value, which is simply the intrinsic hydrogen bonding energy of that

subunit with the subunit(s) to which it attaches. Since the hydrogen bonding interaction of H_2O is intrinsically much higher than NH_3, the convergence can be expected to be relatively slow for hydrated hydronium as compared to ammoniated ammonium.

The υ_3 antisymmetric stretching band for the solvent molecules in $NH_4^+(NH_3)_n$ was first observed in the n=1 cluster. Plotted in Figure 10a are the frequencies of the central $^RQ_0$ bands in the internal rotation structure for this transition as a function of cluster size. Convergence of this plot is observed with increasing n, as is a discontinuity in the curve at the n=5 cluster where the second solvation shell of the system begins to form.

Similar plots for the core vibrational features appear in figures 10b and 10c. Figure 10b shows the position of the ammonium core N-H stretch with attached 1° NH_3 (The first point in this plot, labeled with a square, is from Schwarz's measurement of the n=2 cluster.[38]) Figure 10c shows the position of the bands of the same oscillators with associated 1° and 2° NH_3's. Both of these features converge at large n.

For the hydrogen bonded ionic clusters considered here, there is no precise analogy of the gas phase cluster to the bulk phase, which always contains counter ions. For weak counter ions and/or high molar ratios of solvent to ion core in the bulk, the possibility remains that properties can be somewhat similar at least for portions of the gas phase cluster. The environments of the ion core and innermost solvent shells can be expected to approach their bulk counterparts more closely than outermost solvent shells, especially when the counter ion is excluded from close proximity to the core and inner shell solvent species. The spectrum of n=8, which is quite similar to the spectra of n=9 and 10 in the regions where they overlap, shows definite similarity to the spectra of $NH_4^+ClO_4^-$ in NH_3 with a 1:3 mole ratio.[81] When the ratio of NH_3 is higher, even the salt with the strongly interacting Cl^- counter ion has spectra similar to the gas phase ionic cluster. Most of the vibrational bands show a correspondence which is close enough to assign the solution phase spectra. The most intense band in the solution phase spectrum is centered at about 2800 cm^{-1}, and can be assigned by this means to a vibration of an extensively NH_3 solvated NH_4^+ ion with a mode closely analogous to the intense υ_3 mode of the n=8 ion core. For $n \geq 7$ in the gas phase cluster, $\Delta\nu/\Delta n$ is rather small (see fig. 10c), indicating convergence. For the $NH_4^+ClO_4^-$ in NH_3 with a 1:3 mole ratio, this may mean that NH_4^+ ions are connected by a bridge of NH_3 solvent molecules. It seems that for the large ammoniated ammonium ions, from the standpoint of the ion core and to some extent the first solvent shell, a liquid-like environment is reached by about the n=8 cluster. Of course, the gas phase environment is still much less fluxional - for example, hydrogen bonds are not being continuously broken and reformed.

Hydrated hydronium spectra, even at m=8, show relatively little resemblance to aqueous acid solutions. The larger hydrogen bonding interaction and greater degree of ion-induced structuring evidently dictate comparison with much larger gas phase clusters if one is to see good spectral correspondence.

5.4.6.3 Future Developments:

We have described the spectroscopic study of only a small subset of the ionic clusters that may be probed in the 2.5-3.9 μm region of the spectrum, at lower resolution than what is routinely possible now. Enhanced laser resolution and improved power from newer pulsed dye laser systems makes possible studies of the smaller cluster ions n,m=1-4 at high resolution (< 0.03 cm^{-1}). Studies of this sort should provide fully resolved vibration-rotation spectra for some of these species. Analysis of these spectra will yield improved geometries and provide essential information regarding the position of the proton between solvent molecules, and the degree of distortion that the substituents undergo due to solvent-solvent interactions.

MAMICS is, of course, not limited to the study of hydrogen bonded species; certainly the majority of the hundreds of cluster ions listed in compilations such as Castleman's[2] are amenable to the technique. Spectroscopy of species such as $Na^+(H_2O)_n$ is an obvious development which requires minimal change to the MAMICS apparatus. This species presumably becomes hydrogen bonding after the first solvent shell is filled. While it is somewhat less sensitive, the depletion detection technique of Lisy using a line tunable CO_2 laser has already demonstrated that $Cs^+(CH_3OH)_n$ has a first solvent shell size of n=10.[51] The $(H_2O)_ne^-$ species or hydrated electron is another example of a charged cluster system of considerable chemical interest.

MAMICS is not at all limited to the infrared, and we can envision it being performed from vacuum ultraviolet to 20 μm with resolution and accuracy better than 0.05 cm^{-1}. Nor is MAMICS necessarily limited to the study of the m<500 amu species described in this article. With the use of a more suitable ion source and improved mass analysis, we envision the MAMICS study of large systems, possibly even molecules of biological interest such as solvated peptides of 10,000 amu molecular weight!

Our understanding of the way atoms and molecules are held "by the entanglement of their own interlocking shapes" has been greatly enhanced in recent years by the study of cluster systems. Studying the infrared spectroscopy of ionic clusters has been shown to be a valuable way of learning about the organization of molecules around an ion, and the onset of solution phase properties. The MAMICS technique is a useful method for obtaining this information.

ACKNOWLEDGEMENTS:

The authors would like to thank Dr. Gereon Niedner-Schatteburg for a critical reading of the manuscript. His helpful comments were greatly appreciated.

This work was supported by the Director, Office of Energy Research, Office of Basic Energy Sciences, Chemical Sciences Division of the U.S. Department of Energy, under Contract No. DE-AC03-76SF00098.

TABLE I: $-\Delta H^\circ$ for the Stepwise Solvation of a Number of ions in this work. (Units are in kcal/mol.)

Ref	Ion	Neutral	$-\Delta H^\circ$: $Ion(Neutal)_{n-1}$ + Neutral -> $Ion(Neutral)_n$						
			n=1	2	3	4	5	6	7
a	H_3^+	H_2	9.6	4.1	3.8	2.4			
b	H_3O^+	H_2O	36	22.3	17	15.3	13	11.7	10.3
c	NH_4^+	H_2O	19.9	14.8	12.2	10.8	10.6	9.1	8.4
d	$NH_4^+(NH_3)$	H_2O	12.9	12.7	12.2				
d	$NH_4^+(NH_3)_2$	H_2O	12.4	11.7					
d	$NH_4^+(NH_3)_3$	H_2O	11.7						
e	NH_4^+	NH_3	27	17	16.5	14.5	7.5		
f	NH_4^+	NH_3	21.5	16.2	13.5	11.7	7.0	6.5	

a. K. Hiraoka and P. Kebarle, J. Chem. Phys. **62**, 2267 (1975).
b. P. Kebarle, S.K. Searles, A. Zolla, J. Scarborough, and M. Arshadi, J. Am. Chem. Soc. **89**, 6393 (1967).
c. M. Meot-Ner, J. Am. Chem. Soc. **106**, 1265 (1984).
d. J.D. Payzant, A.J. Cunningham, and P. Kebarle, Cand.J. Chem. **51**, 3242 (1973).
e. S.K. Searles, and P. Kebarle, J. Phys. Chem. **72**, 742 (1968).
f. M.R. Ashardi and J.H. Futrell, J. Phys. Chem. **78**, 1482 (1974).

TABLE IIa: Molecular Constants for NH_4^+, and NH_3.
(All units are in cm^{-1} except ζ_3 which is dimensionless.)

Molecule or Ion:	Symmetry	Molecular Constants:	Reference
NH_4^+	T_d	υ_1: 3270 ± 25	a
		υ_2: 1669	c
		υ_3: 3343.26	e
		υ_4: 1447.22	f
		A_o: 5.9293 ± 0.0002	e
		B_o: "	e
		C_o: "	e
		ζ_3: 0.0604	e
NH_3	C_{3v}	υ_1: 3336.2,3337.2	b,g
		υ_2: 932.5,968.3	d,g
		υ_3: 3443.6,3443.9	d,g
		υ_4: 1626.1,1627.4	d,g
		A_o: 6.196	g
		B_o: 9.444	g
		C_o: "	g
		ζ_3: 0.06	g

a. P. Botschwina, J. Chem. Phys. **87**, 1453 (1987), scaled ab initio value.
b. W.S. Benedict, E.K. Plyler and E.D. Tidwell, J. Chem. Phys. **32**, 32 (1960).
c. D.J. DeFrees and A.D. McLean, J. Chem. Phys. **82**, 333 (1985), scaled ab initio value.
d. T. Shimanouchi, Tables of Molecular Vibrational Frequencies, U.S. Dept. of Commerce, Natl. Stand. Ref. Data Ser. Natl. Bur. Stand. **39** (U.S. GPO, Washington, D.C., 1972).
e. M.W. Crofton, and T. Oka, J. Chem. Phys. **79**, 3157 (1983); **86**, 5983 (1987).
f. M. Polak, M. Gruebele, B.W. DeKock and R.J. Saykally, Mol. Phys. **66**, 1193 (1989).
g. G. Herzberg, Electronic spectra of Polyatomic Molecules (Van Nostrand, Princeton, N.J., 1967).

TABLE IIb: Molecular Constants for H_3O^+ and H_2O.
(All units are in cm^{-1} except ζ which is dimensionless.
Rotational constants are for the ground vibrational state.)

Molecule or Ion:	Symmetry	Molecular Constants:	Reference
H_3O^+	C_{3v}	υ_1: 3570	a
		υ_2: 954.40 ($1^- \leftarrow 0^+$)	b
		υ_2: 525.83 ($1^+ \leftarrow 0^-$)	b
		υ_3: 3530.17,3513.84	c
		υ_4: 1564	a
		$A_o=B_o$: 11.2540 (0^+)	b
		C_o: 6.1	c
H_2O	C_{2v}	υ_1: 3656.7	d
		υ_2: 1594.6	d
		υ_3: 3755.8	d
		A: 27.877	e
		B: 14.512	e
		C: 9.285	e

a. P.R. Bunker, W.P. Kraemer and V. Špirko, J.Molec. Spec. **101**, 180 (1983). -- Scaled ab initio value.
b. D-J. Liu, T. Oka, and T.J. Sears, J. Chem. Phys. **84**, 1312 (1986); and references therein.
c. M.H. Begemann, G.S Gudeman, J. Pfaff, and R.J. Saykally, Phys. Rev. Lett. Vol. 51, 554 (1983); M.H. Begemann and R.J. Saykally: J. Chem. Phys. **82**, 3570 (1985).
d. W.S. Benedict, N. Gailar, and E.K. Plyler, J. Chem. Phys. **24**, 1139 (1956).
e. G. Herzberg, Electronic spectra of Polyatomic Molecules (Van Nostrand, Princeton, N.J., 1967).

REFERENCES:

1. T.L. Carus, On the Nature of the Universe, trans. R.E. Latham, Ed. B. Radice (New York: Penguin Books, 1956).

2. R.G. Keesee and A.W. Castleman, Jr. J. Phys. Chem. Ref. Data, Vol. 15, No. 8 (1986).

3. See Refs. 17, 19, and 23.

4. J.V. Coe, and R.J. Saykally, " Infrared Laser Spectroscopy of Molecular Ions" in Ion and Cluster Ion Spectroscopy and Structure, ed. J.P. Maier (Elsevier, Amsterdam, 1989).

5. H. Heitmann, and F. Arnold, Nature **306**, 747 (1983).

6. R.S. Narcisi and A.D. Bailey, J. Geophys. Res. **70**, 3687 (1965).

7. E.E. Ferguson, F.C. Fehsenfeld, and D.L. Albritton, in Gas Phase Ion Chemistry, vol. 1, M.T. Bowers, ed. (Academic Press, New York, 1979).

8. Smith, D.S. and Adams, N.G., Top. Curr. Chem. **89**, 1 (1980); Keesee, R.G. and Castleman, A.W. Jr., J. Geophys. Res. **90**, 5885 (1985).

9. Castleman, A.W. Jr., Holland, P.M., and Keesee, R.G., J. Chem. Phys. **68**, 1760 (1978); Castleman, A.W. Jr., Adv. Colloid and Interface Science **10**, 73 (1979).

10. Heinis, T., Chowdhury, S., Scott, S.L., and Kebarle, P., J. Am. Chem. Soc. **110**, 400 (1988); Grese, R.P., Cerny, R.L., and Gross, M.L.,: **111**, 2835 (1989).

11. Y.K. Lau, S. Ikuta, and P. Kebarle, J. Am. Chem. Soc. **104**, 1462 (1982); A.J. Cunningham, J.D. Payzant, and P. Kebarle **94**, 7627 (1972); P. Kebarle, S.K. Searles, A. Zolla, J. Scarborough, and M. Arshadi, **89**, 6393 (1967).

12. M. Meot-Ner and F.H. Field, J. Am. Chem. Soc. **99**, 998 (1977).

13. J.C. Gary and P. Kebarle, J. Phys. Chem. **94**, 5184 (1990).

14. M. Meot-Ner, L.W. Sieck, J. Phys. Chem. **90**, 6687 (1986); L.W. Sieck, J. Phys. Chem. **89**, 5552 (1985).

15. I. Dzidic and P. Kebarle, J. Phys. Chem. **74**, 1466 (1970).

16. Alcami, M., Mo, O., Yanez, M., Anvia, F., and Taft, R.W.: J. Phys. Chem. 94, 4796 (1990).

17. "Calculated Vibrational Spectra of Hydrogen Bonded Systems" by P. Janoschek in The Hydrogen Bond, vol. I, ed. by P. Schuster, G. Zundel and C. Sandorfy (North-Holland, New York), 1976, p.183.

18. The Hydrogen Bond Vols. I, II, and III, ed., P. Schuster, G. Zundel and C. Sandorfy, (North-Holland Publishing, Amsterdam 1976).

19. S. Scheiner, Acc. Chem. Res. **18**, 174 (1985), and references therein.

20. R.A. Copeland, and S.I. Chan, Annu. Rev. Phys. Chem. **40**, 671 (1989); F.M. Koswer and D. Huppert, Annu. Rev. Phys. Chem. **37**, 127 (1986).

21. G.C. Pimentel M.O. Bulanin and M. Van Theil, J. Chem. Phys. **36**, 500 (1962).

22. Caldin, E.F., Gold, V., eds.: Proton Transfer Reactions (Chapman and Hall, London), 1975.

23. C.I. Ratcliffe and D.E. Irish, in Water Science Reviews 2, ed. by F. Franks (Cambridge University Press, Cambridge 1986).

24. J. Corset, P.V. Huong and J. Lascombe, Spectrochim. Acta A **24**, 2045 (1968).

25. D.D. Nelson, Jr., G.T. Fraser and W. Klemperer, J. Chem. Phys. **83**, 6201 (1985).

26. Water Science Reviews 3 , F. Franks, ed. (Cambridge University Press, Cambridge 1988).

27. T.R. Dyke and J.S. Muenter, J. Chem. Phys. **57**, 5011 (1972); Z.S. Hyang and R.E. Miller, J. Chem. Phys. **88**, 8008 (1988).

28. K.L. Busarow, R.C. Cohen, G.A. Blake, K.B. Laughlin, Y.T. Lee, and R.J. Saykally, J. Chem. Phys. **90**, 3937 (1989).

29. L.H. Coudert, and J.T. Hougen, J. Mol. Spectr. **130**, 86 (1988); L.H. Coudert, F.J. Lovas, R.D. Suenram and J.T. Hougen, J. Chem. Phys. **87**, 6290 (1987); J.T. Hougen, J. Mol. Spectr. **114**, 395 (1985).

30. S.E. Novick, K.R. Leopold, and W. Klemperer, The Structures of Weakly Bound Complexes as Elucidated by Microwave and Infrared Spectroscopy, ed. by E.R. Bernstein (Elsevier, New York, 1989).

31. R.E. Miller, J. Phys. Chem. **90**, 3301 (1986); Structure and Dynamics of Weakly Bound Molecular Clusters, ed. by A. Weber, NATO ASI Series (Reidel, Dordrecht, 1987); D.J. Nesbitt, Chem. Rev. **88**, 843 (1988); M.A. Duncan and D.H. Rouvray, Sci. Am. **261**, 110 (1989).

32. M.F. Vernon, Ph.D. Thesis, University of California, Berkeley, 1982.

33. M.F. Vernon, D.J. Krajnovigh, H.S. Kwok, L.M. Lisy, Y.R. Shen, and Y.T. Lee, J. Chem. Phys. **77**, 47 (1982).

34. R.H. Page, M.F. Vernon, Y.R. Shen and Y.T. Lee, Chem. Phys. Lett. Vol. 141, No. 1,2, 1 (1987).

35. D.F. Coker, R.E. Miller, and R.O. Watts, J. Chem. Phys. **82**, 3554 (1984).

36. Buck, U.; and Lauenstein, C.: J. Chem. Phys. 92, 4250 (1990).

37. Gudeman, C.S. and Saykally, R.J.,: Ann. Rev. Phys. Chem. **35**, 387 (1984).

38. H.A. Schwarz, J. Chem. Phys., **67**, 5525 (1977).

39. H.A. Schwarz, J. Chem. Phys. **72**, 284 (1980).

40. Crofton, M.W.; Jagod, M.-F.; Rehfuss, B.D.; and Oka, T.: J. Chem. Phys. 91, 5139 (1989).

41. W.H. Wing, G.A. Ruff, W.E. Lamb Jr., and J.J. Spezeski, Phys. Rev. Lett. **36**, 1488 (1976); and ongoing experiments in the R.J. Saykally laboratory at University of California, Berkeley.

42. Levinger, N.E., Ray, D., Alexander, M.L., and Lineberger, W.C.,: J. Chem. Phys. **89**, 5654 (1988).

43. L.A. Posey and M.A. Johnson, J. Chem. Phys. **89**, 4807 (1988); M.J. DeLuca, B. Niu, and M.A. Johnson, J. Chem. Phys. **88**, 5857 (1988).

44. J.T. Snodgrass, J.V. Coe, C.B. Freidhoff, K.M. McHugh and K.H. Bowen, J. Chem. Phys. **88**, 8014 (1988).

45. C.Y. Kung and T.A. Miller, J. Chem. Phys. **92**, 3297 (1990).

46. J.P. Maier, ed.: Ion and Cluster Ion Spectroscopy and Structure (Elsevier, Amsterdam, 1989).

47. Steadman, J. and Syage, J.: J. Chem. Phys. 92, 4630 (1990); Breen, J.J.; Peng, L.W.; Willberg, D.M.; Heikal, A.; Cong, P.; and Zewail, A.H.: J. Chem. Phys. 92, 805 (1990).

48. M. Okumura, L.I. Yeh, and Y.T. Lee, J. Chem. Phys. **88**, 79 (1988).

49. L.I. Yeh, M. Okumura, J.D. Myers, J.M. Price, and Y.T. Lee, J.Chem. Phys. **91**, 7319 (1989).

50. M. Okumura, L.I. Yeh, J.D. Meyers and Y.T. Lee, J. Phys. Chem., **94**, 3416 (1990).

51. W-L. Liu, and J.M. Lisy, J. Chem. Phys. **89**, 605 (1988); J.A. Draves, Z. Luthey-Schulten, W-L. Liu and J.M. Lisy, Submitted J. Chem. Phys. (1990).

52. Bjorklund, G.C.: Opt. Lett. 5, 15 (1980); Nesbitt, D.J.; Petek, H.; Gudeman, C.S.; Moore, C.B.; and Saykally, R.J.: J. Chem. Phys. 81, 5281 (1984).

53. See ref. 40.

54. M. Okumura, Ph.D. Thesis, University of California, Berkeley (1986).

55. L.I. Yeh, Ph.D. Thesis, University of California, Berkeley (1988); Engleking, P.C.: Rev. Sci. Instrum. 57, 2274 (1986).

56. E. Teloy and D. Gerlich, Chem. Phys. **4**, 417 (1974); D. Gerlich in, Electronic and Atomic Collisions ed. D.C. Lorents, W.E. Meyerhof and J.R. Peterson, (North-Holland press, Amsterdam 1985).

57. M. Okumura, L.I. Yeh and Y.T. Lee, J. Chem. Phys. **83**, 3705 (1985); **88**, 79 (1988).

58. J.M. Price, M.W. Crofton and Y.T. Lee, J. Chem. Phys. **91**, 2749 (1989); J.M. Price, M.W. Crofton and Y.T. Lee, J. Phys. Chem., Accepted (1990).

59. Crofton, M.W. and Oka, T.: J. Chem. Phys. 79, 3157 (1983); 86, 5983 (1987).

60. Schafer, E. and Saykally, R.J.: J. Chem. Phys. 79, 3159 (1983); Schafer, E.; Saykally, R.J.; and Robiette, A.G.: J. Chem. Phys. 80, 3969 (1984).

61. W. S. Benedict, E. K. Phyler, and E. D. Tidwell, J. Chem. Phys. **32**, 32 (1960).

62. M.W. Crofton, J.M. Price, and Y.T. Lee, "Infrared Spectroscopy of the Hydrated Hydronium Ions, $H_3O^+(H_2O)_m$ (m=3-8)", to be submitted to J. Chem. Phys. (1990).

63. Jorgensen, W.L.,: J. Am. Chem. Soc. **103**, 341 (1981); Chandrasekhar, J. and Jorgensen, W.L.,: J. Chem. Phys. **77**, 5080 (1982).

64. E. Kochanski,: J. Am. Chem. Soc. **107**, 7869 (1985).

65. Malenkov, G.G.: "The Chemical Physics of Solvation," in Studies in Physical and Theoretical Chemistry, ed. by R.R. Dogonadze, E. Kalman, A.A. Kornyshev, and J. Ulstrup (Elsevier, New York, 1984).

66. DeRaedt, B., Sprik, M., and Klein, M.L.,: J. Chem. Phys. **80**, 5719 (1984); Impey, R.W., Sprik, M., and Klein, M.L.,: J. Am. Chem. Soc. **109**, 5900 (1987).

67. Mezei, M. and Beveridge, D.L.,: J. Chem. Phys. **74**, 6902 (1981); Rao, M. and Berne, B.J.,: J. Phys. Chem. **85**, 1498 (1981).

68. R. Remington and H.F. Schaefer III., unpublished results.

69. M.D. Newton, J. Chem. Phys., **67**, 5535 (1977).

70. M.D. Newton, S. Ehrenson, J. Am. Chem. Soc. **93**, 4971 (1971).

71. See refs. 32-35.

72. J.M. Price, M.W. Crofton and Y.T. Lee, "Infrared Spectroscopy of the $NH_4^+(NH_3)_n(H_2O)_m$ Ionic Clusters", to be Submitted, J. Chem. Phys. (1990).

73. S.G. Lias, J.F. Liebman and R.D. Levin, J. Phys. Chem. Ref. Data **13**, 695 (1984).

74. A. Pullman and A.M. Armbruster, Chem. Phys. Lett. **36**, 558 (1975); Intern. J. Quantum Chem. **8S**, 169 (1974).

75. Cazzoli, G.;Favero, P.G.; Lister, D.G.; Legon, A.C.; Millen, D.J.; and Kisiel, Z.: Chem. Phys. Lett. **117**, 543 (1985), and references contained therein.

76. McKellar, A.R.W.: J. Chem. Phys. **93**, 18 (1990), and references contained therein.

77. G.T. Fraser, K.R. Leopold, and W. Klemperer, J. Chem. Phys. **81**, 2577 (1984), see also: K.I. Peterson, and W. Klemperer, J. Chem. Phys. **80**, 2439 (1983); **85**, 725 (1986).

78. Okumura, M.; Chan, M.-C.; Oka, T.: Phys. Rev. Lett. **62**, 32 (1989); van Kranendonk, J.; Solid Hydrogen (Elsevier, Amsterdam, 1983).

79. W.B. Olson and D. Papousek, J. Mol. Spectr. **37**, 527 (1971), and references contained therein.

80. Townes, C.H; and Schawlow, A.L.: Microwave Spectroscopy (McGraw-Hill, New York, 1955); Owen, N.L.: "Studies of Internal Rotation by Microwave Spectroscopy" in Internal Rotation in Molecules, ed. by Orville-Thomas, W.J. (Wiley, New York, 1974).

81. J. Corset, P.V. Huond and J. Lascombe, Spectrochim. Acta A **24**, 2045 (1968).

FIGURE CAPTIONS:

1. Schematic diagram of the experimental apparatus.

2. Schematic diagram of the ion source, which consists of a corona discharge and supersonic expansion.

3a. The normal vibrations of tetrahedrally symmetric NH_4^+. υ_3 and υ_4 are three fold degenerate, while υ_1 and υ_2 are one and two fold degenerate, respectively. Arrows in the figure indicate the direction of motion but are not to scale with the amplitudes.

3b. Normal modes of NH_3 or H_3O^+. Only one linear combination has been shown for the doubly degenerate modes υ_3 and υ_4. Again, arrows in the figure indicate the direction of motion but are not to scale for the amplitude of the motion.

3c. Normal modes of H_2O. Again, arrows in the figure indicate the direction of motion but are not to scale with the amplitudes.

4. Vibrational predissociation spectra of $NH_4^+(NH_3)_n$ (n=3-8 for 4a-4f, respectively) in the 2600-3500 cm^{-1} region. Bands forming clear series in n are connected by dashed lines.

5. Vibrational predissociation spectra of $NH_4^+(NH_3)_n$ (n=1-6 for 5a-5f, respectively) in the 3370-3470 cm^{-1} region, showing the internal rotation subbands. 6g is the same region for the n=8 cluster which does not show the internal rotation structure. (Due to poor signal to noise, a larger wavelength increment was used in scan 6g than for the scans in 6a-f, but averaging time was increased.) The notation is discussed in the text. Corresponding subbands are connected by solid lines.

6. Proposed structures for the n=4,5 and 8 complexes. The hydrogen bonds are denoted by dashed lines. It is not certain that the hydrogen bonding between 1° and 2° NH_3 is linear.

7. Vibrational predissociation spectra of $H_3O^+(H_2O)_m$ (m=2-8 for 7a-7f, respectively) in the 2600-4000 cm^{-1} region. Bands forming a clear series in m are connected by dashed lines. Structures are observed, supporting the notion that the first solvation shell is filled at m=3, and that the third shell may start to fill before the second shell is full.

8. Vibrational predissociation spectrum for the $NH_4^+(NH_3)_3(H_2O)$ mixed cluster species in the 2600-4000 cm^{-1} region. Bands are observed due to the water, ammonia and ammonium subunits. At least three different isomers are possible, shown above the figure.

9. Simulated and experimental spectrum of $N_2H_7^+$ for the D_{3h} equilibrium structure. The simulation includes only Q branch transitions, since these are expected to dominate the spectrum. Rotational constants used in the simulation: $A'=3.20cm^{-1}$, $A''=3.16cm^{-1}$, $B'=B''=0.16cm^{-1}$, T=30K, $_{\Delta}V=-1.0$, $\zeta=0.0$.

10a. Plot of the $^RQ_0$ bands for the internal rotation structure associated with the 1^0 NH_3's antisymmetric stretching transition as a function of cluster size.

10b. Plot of the peak intensity of the antisymmetric stretching band for the ammonium ion core bound only to 1° NH_3 molecules as a function of cluster size. The series shows eventual convergence as n increases. See text for discussion.

10c. Plot of the peak intensity of the antisymmetric stretching band for the ammonium ion core bound to both 1° and 2° NH_3 molecules as a function of cluster size. Converged values are similar to those observed for some solutions of ammonium salts dissolved in liquid ammonia. See text for discussion.

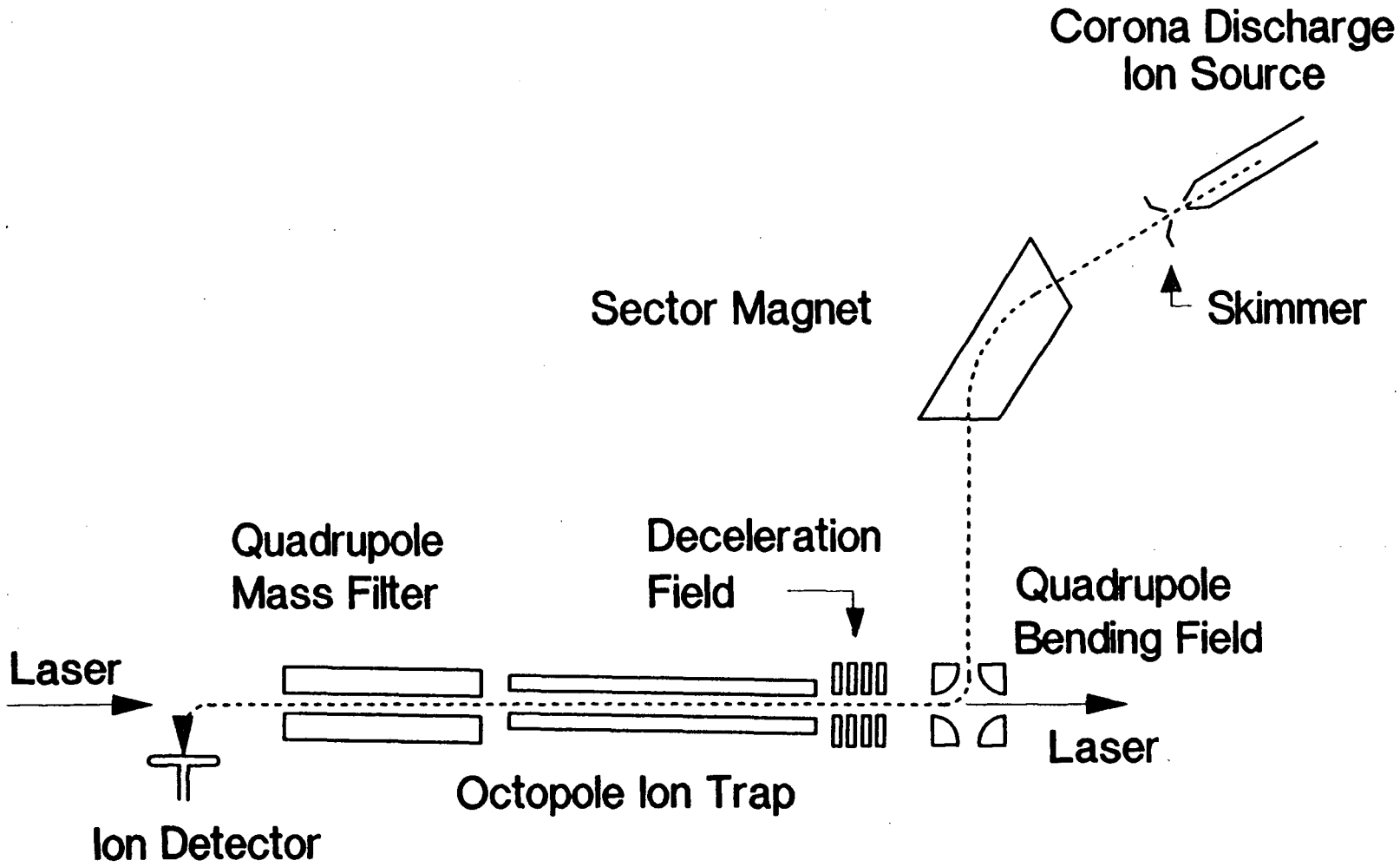
Corona Discharge
Ion Source
Sector Magnet
Skimmer
Quadrupole
Mass Filter
Deceleration
Field
Quadrupole
Bending Field
Laser
Laser
Octopole Ion Trap
Ion Detector

Fig. 1

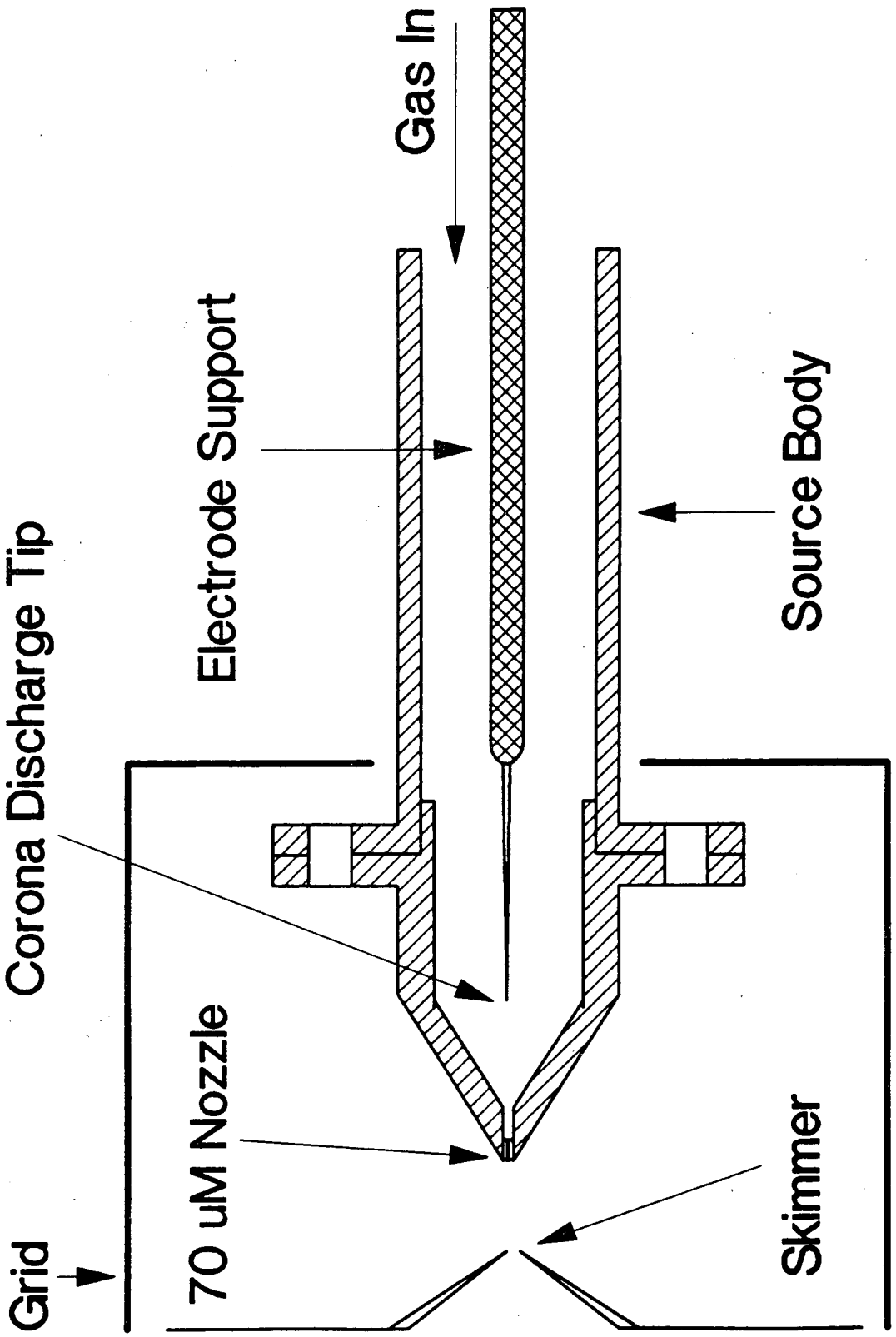
Grid
Corona Discharge Tip
70 uM Nozzle
Electrode Support
Gas In
Source Body
Skimmer

Fig. 2

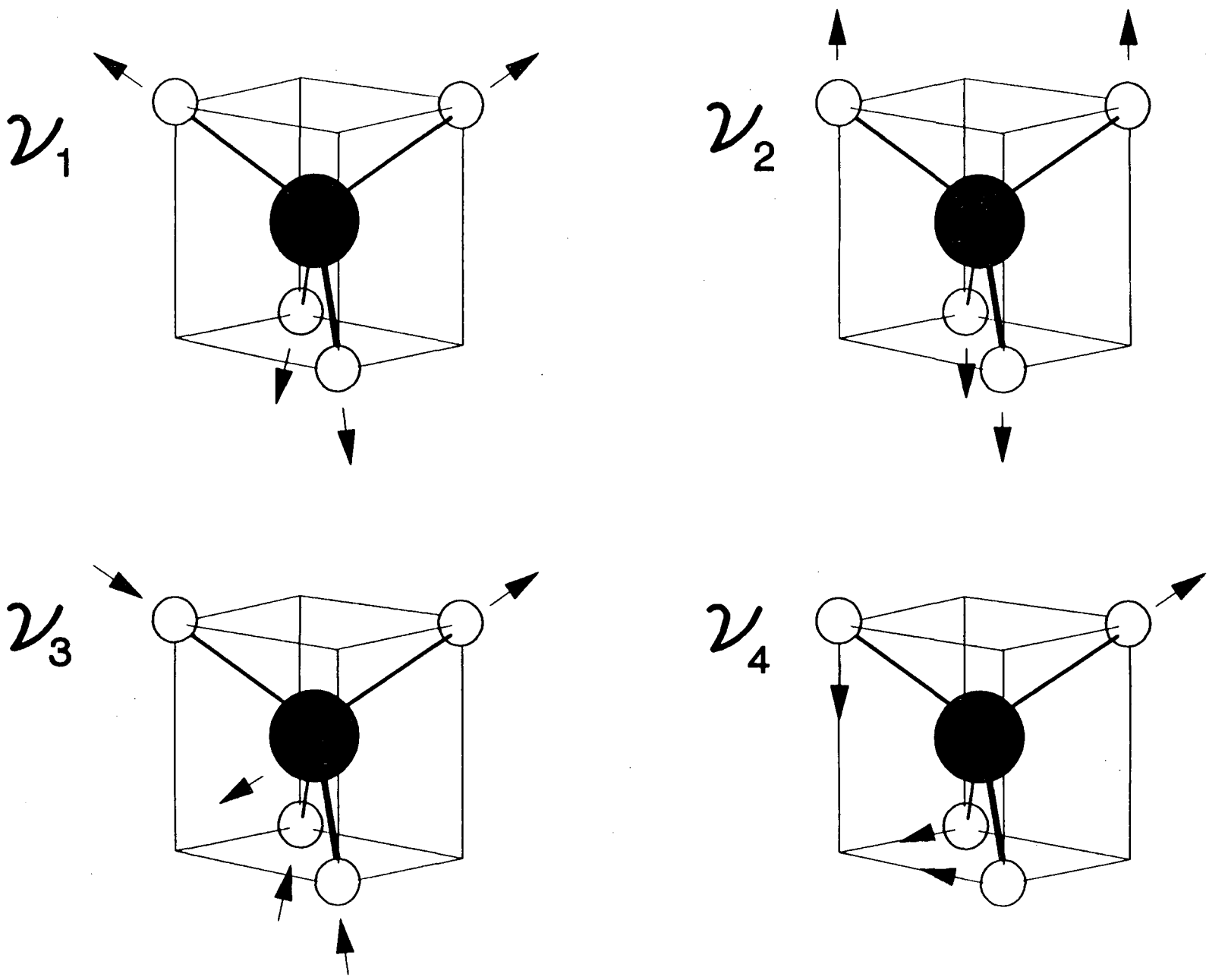

Fig. 3(a)

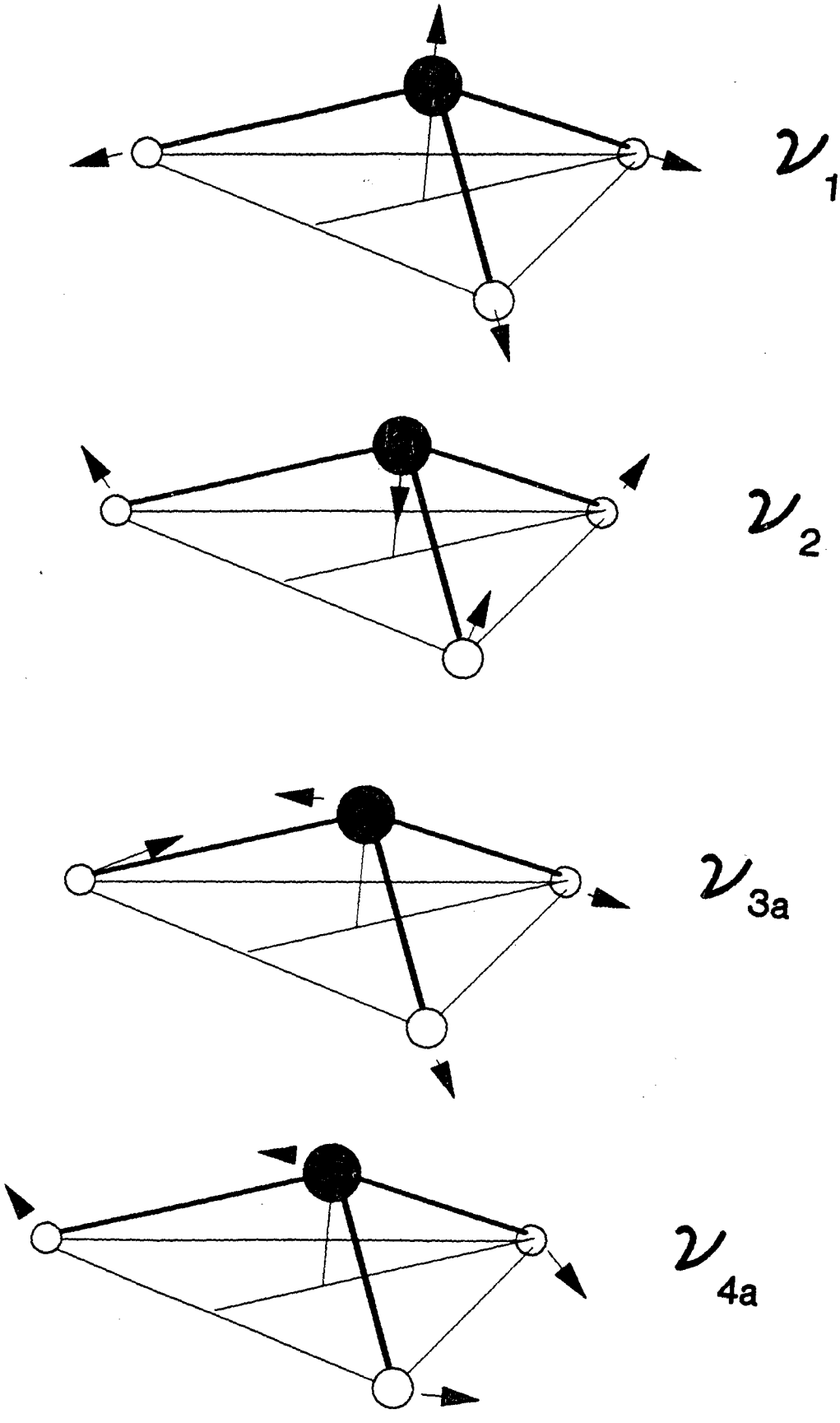

Fig. 3(b)

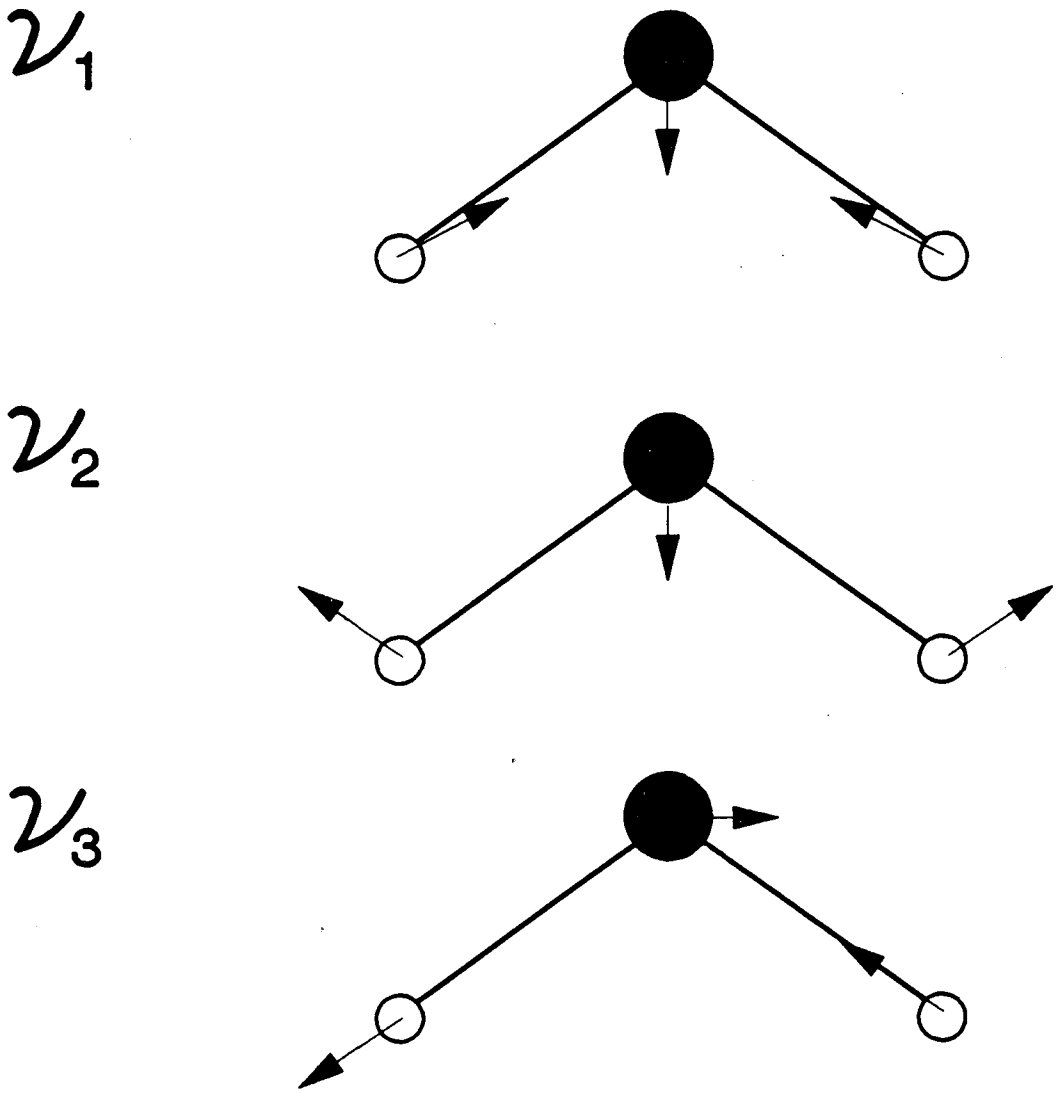

Fig. 3(c)

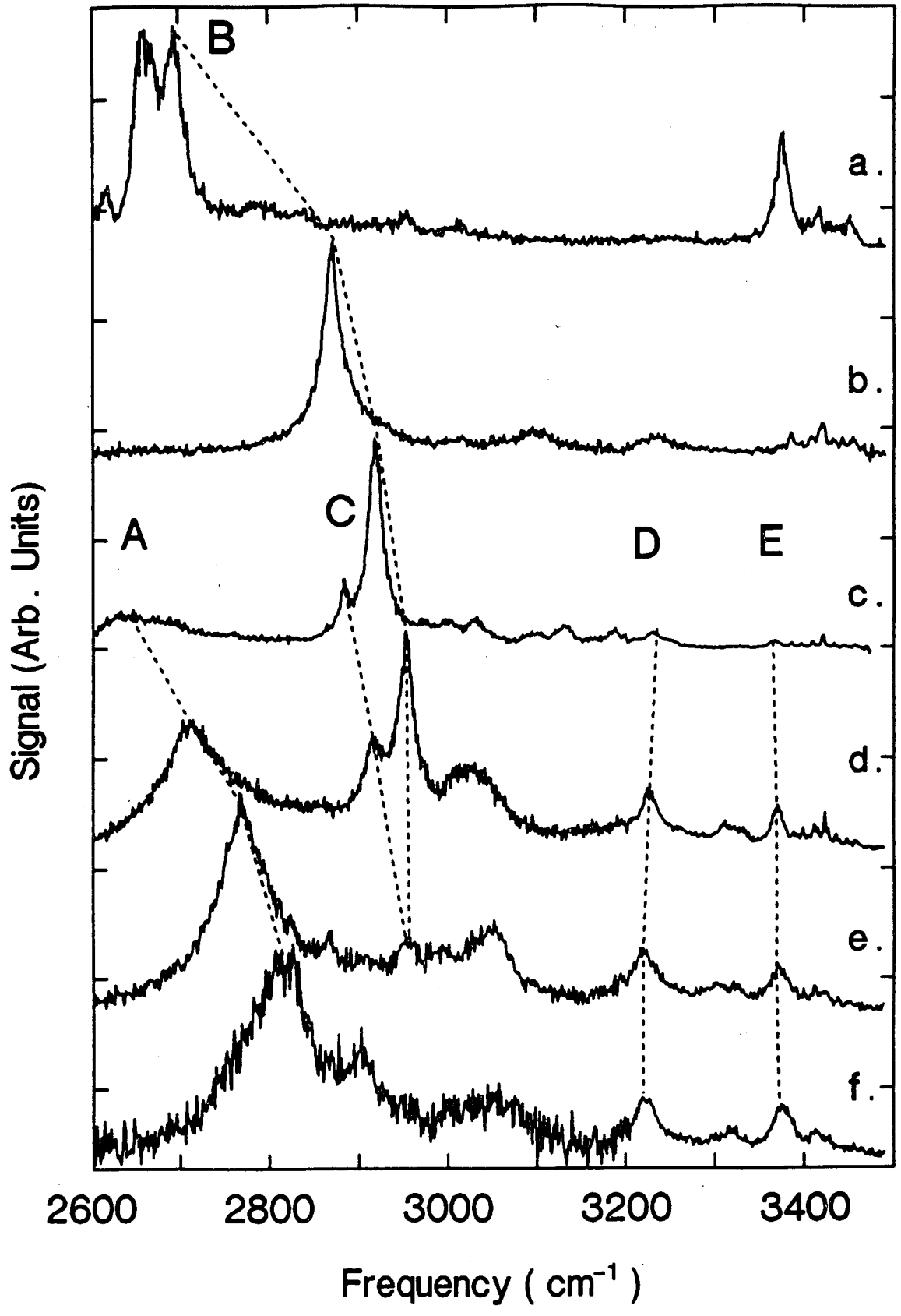
B
a.
b.
A
C
D
E
c.
d.
e.
f.
Signal (Arb. Units)
2600
2800
3000
3200
3400
Frequency (cm^{-1})

Fig. 4

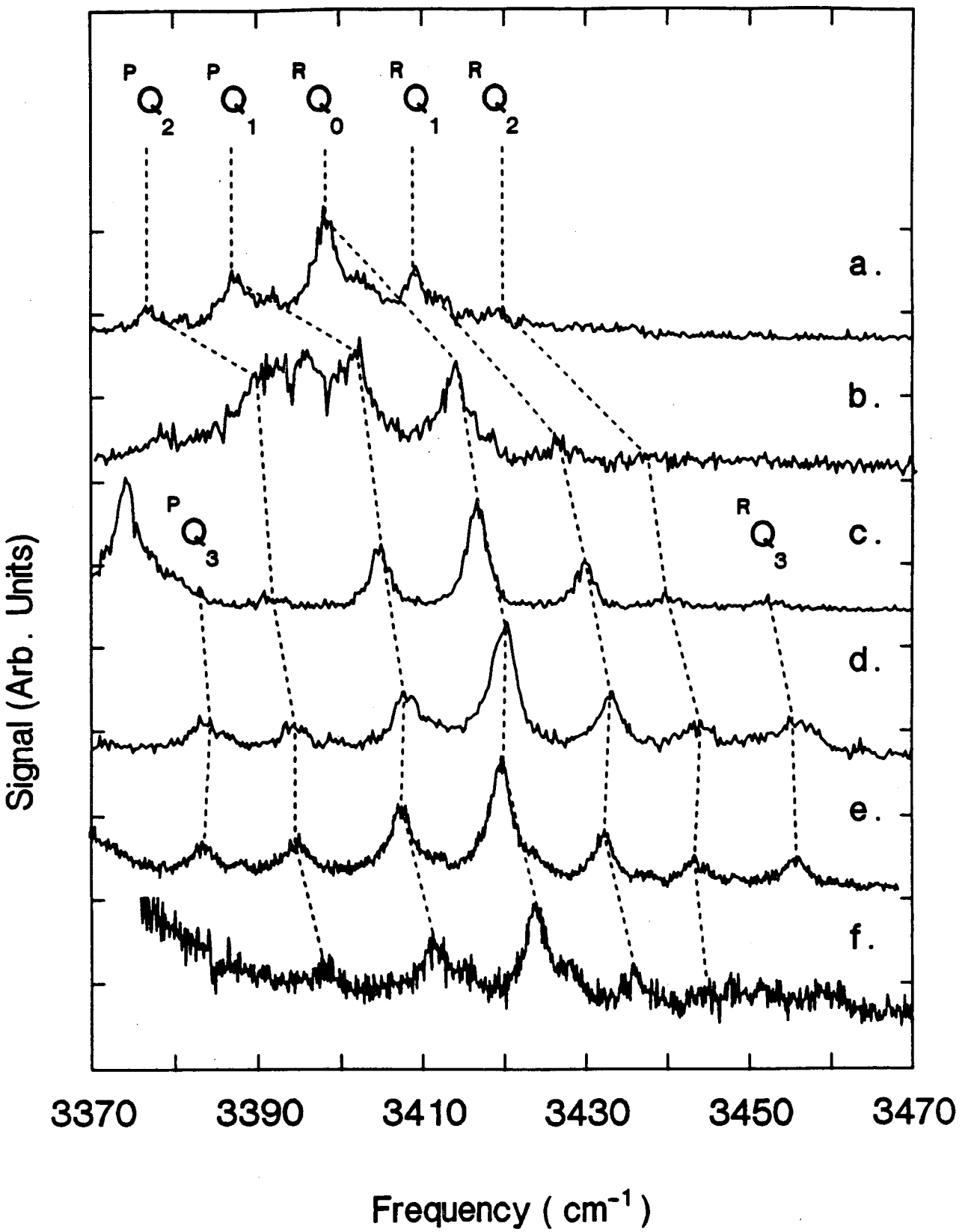
P Q2
P Q1
R Q0
R Q1
R Q2
a.
b.
P Q3
R Q3
c.
d.
e.
f.
Signal (Arb. Units)
3370
3390
3410
3430
3450
3470
Frequency (cm-1)

Fig. 5

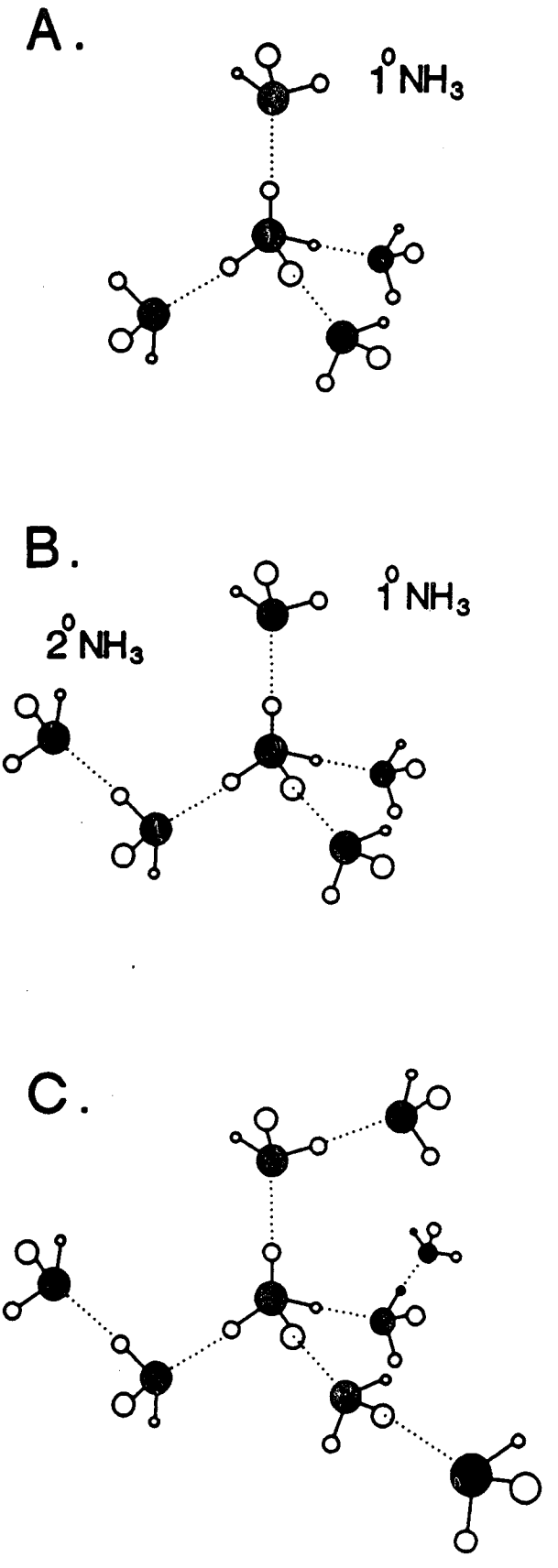

Fig. 6

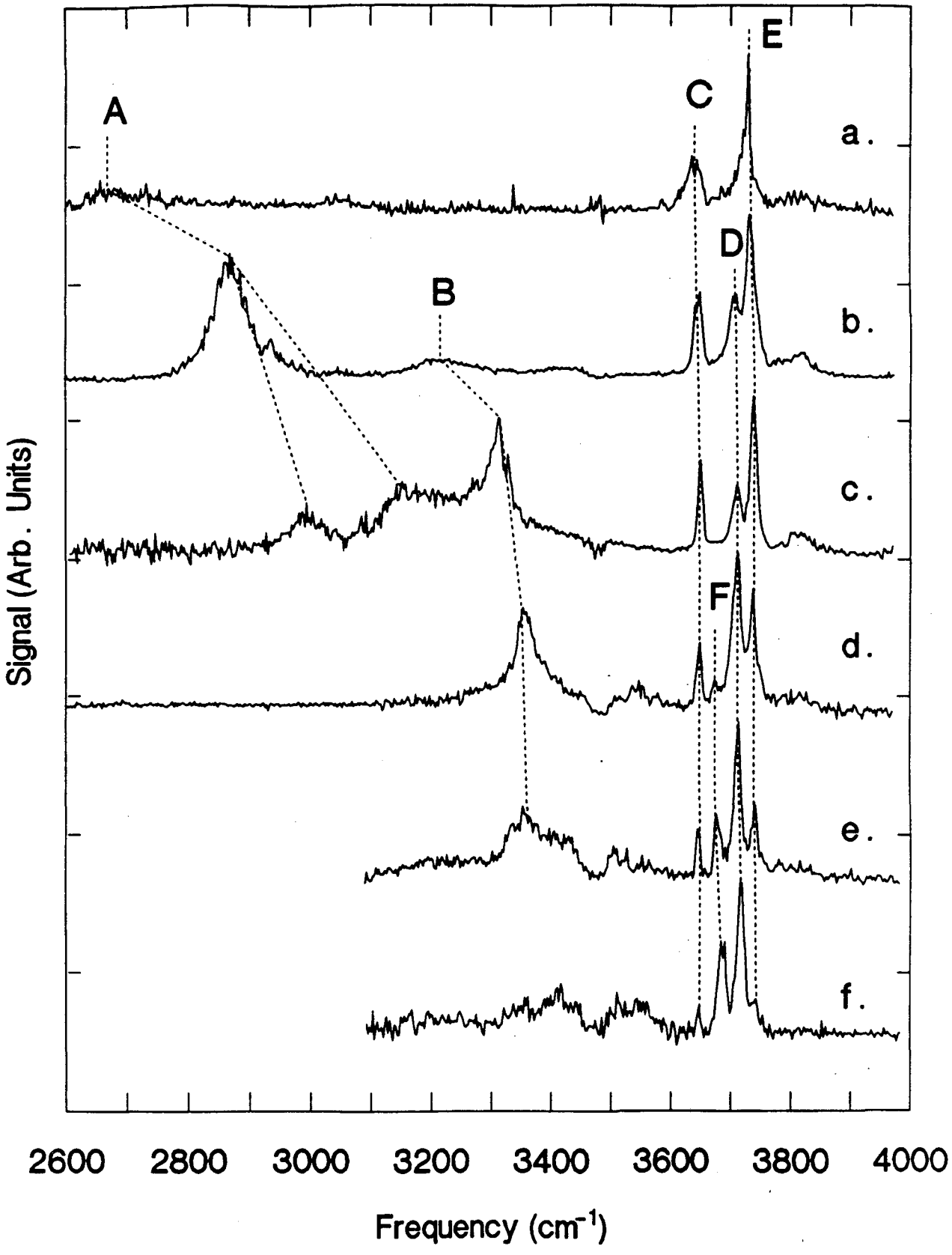
A
B
C
D
E
F
a.
b.
c.
d.
e.
f.
Signal (Arb. Units)
2600
2800
3000
3200
3400
3600
3800
4000
Frequency (cm-1)

Fig. 7

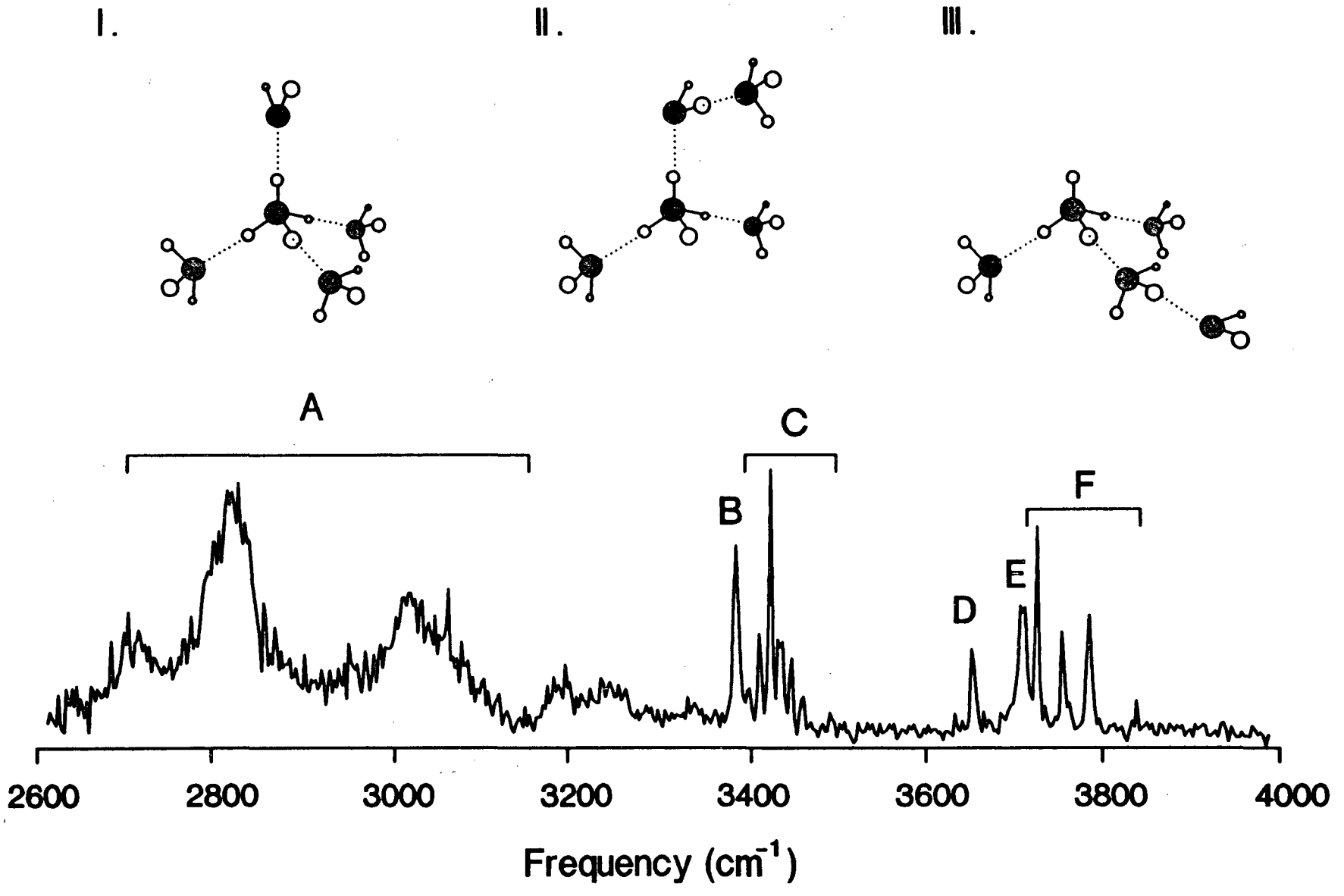
I.
II.
III.
A
B
C
D
E
F
2600
2800
3000
3200
3400
3600
3800
4000
Frequency (cm-1)

Fig. 8

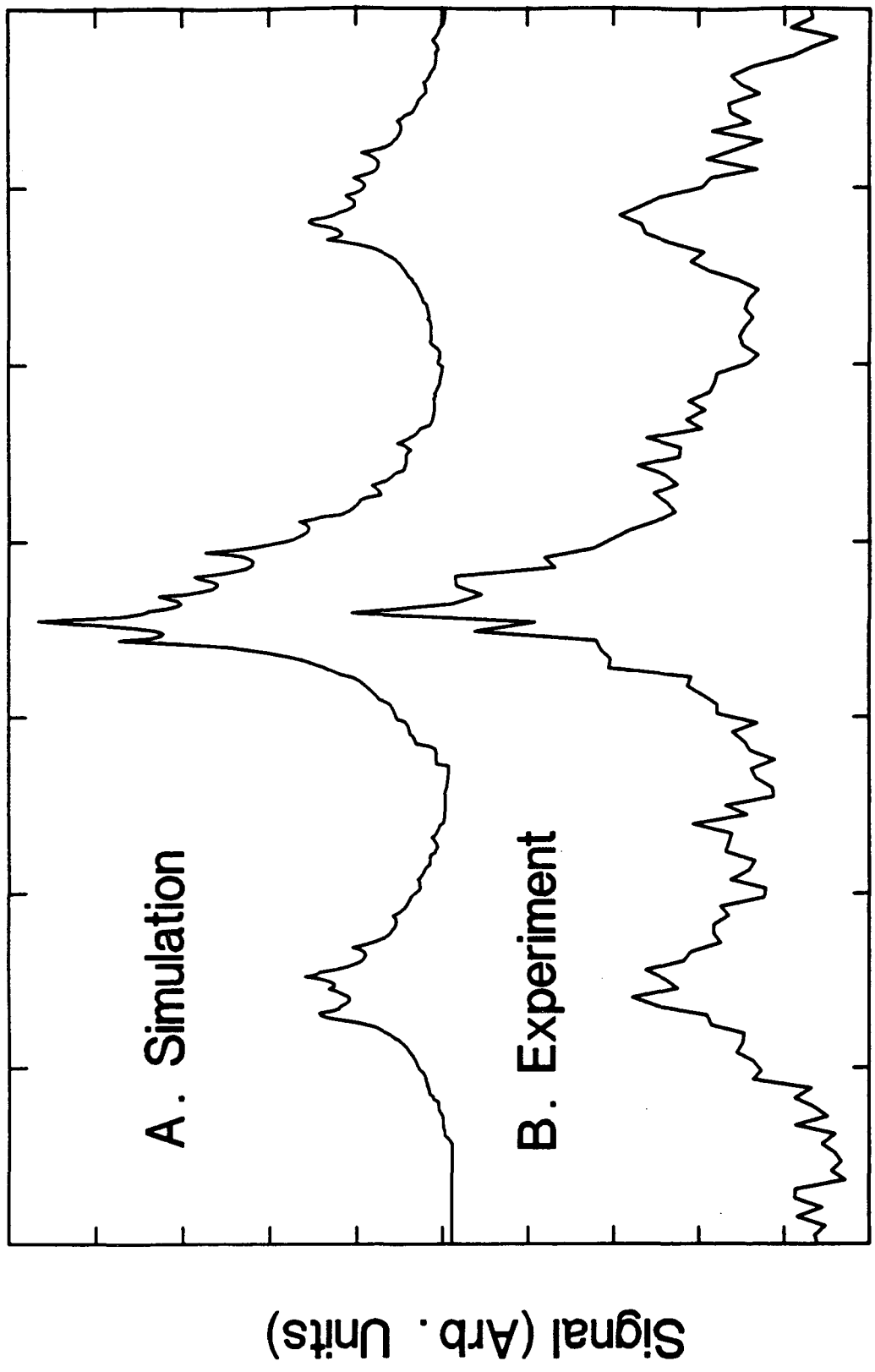
A. Simulation
B. Experiment
3380
3390
3400
3410
Frequency (cm^{-1})
Signal (Arb. Units)

Fig. 9

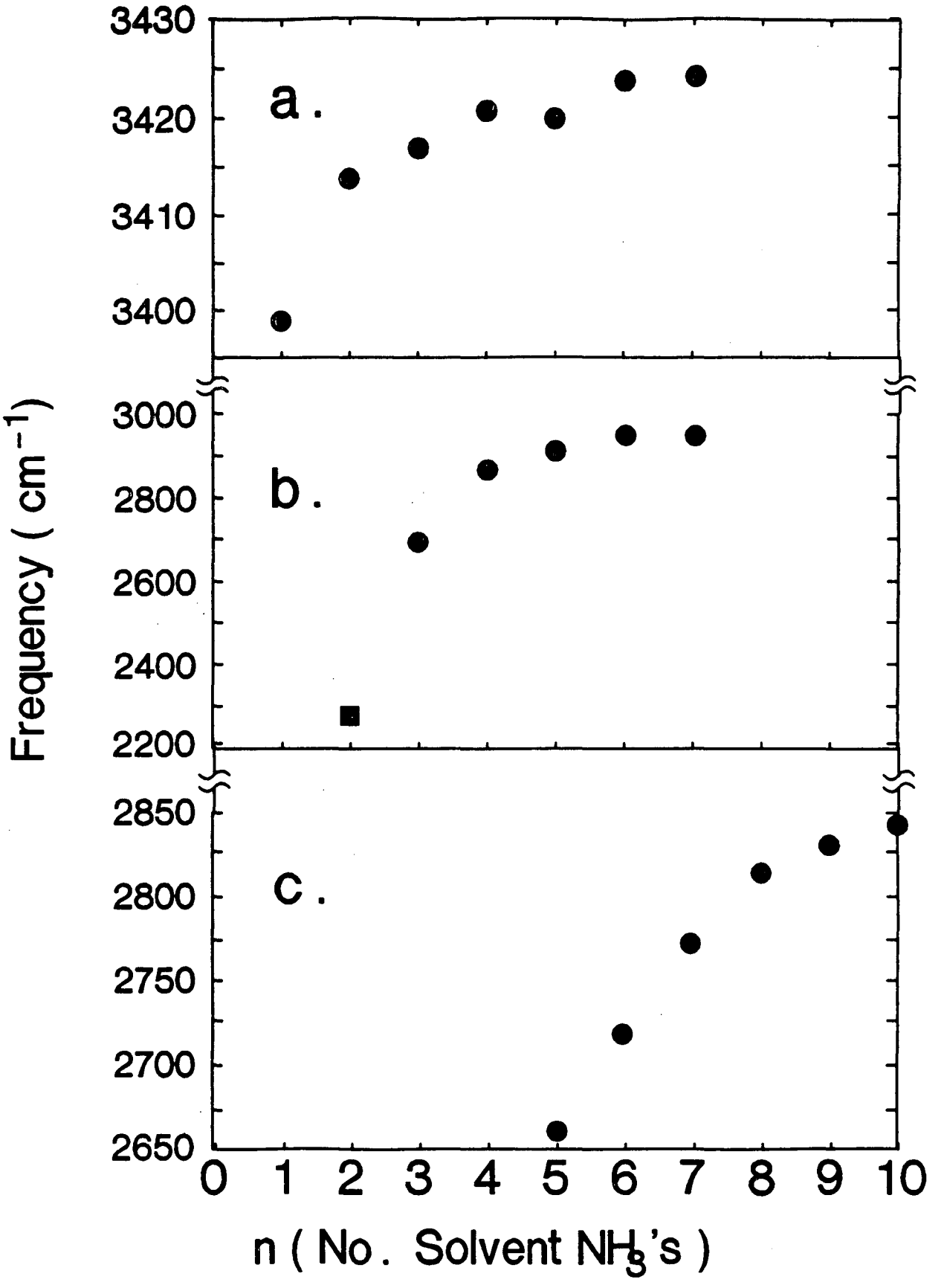
3430
3420
3410
3400
a.
3000
2800
2600
2400
2200
b.
2850
2800
2750
2700
2650
c.
Frequency (cm^{-1})
0 1 2 3 4 5 6 7 8 9 10
n (No. Solvent NH$_3$'s)

Fig. 10(a-c)

LAWRENCE BERKELEY LABORATORY
UNIVERSITY OF CALIFORNIA
INFORMATION RESOURCES DEPARTMENT
BERKELEY, CALIFORNIA 94720